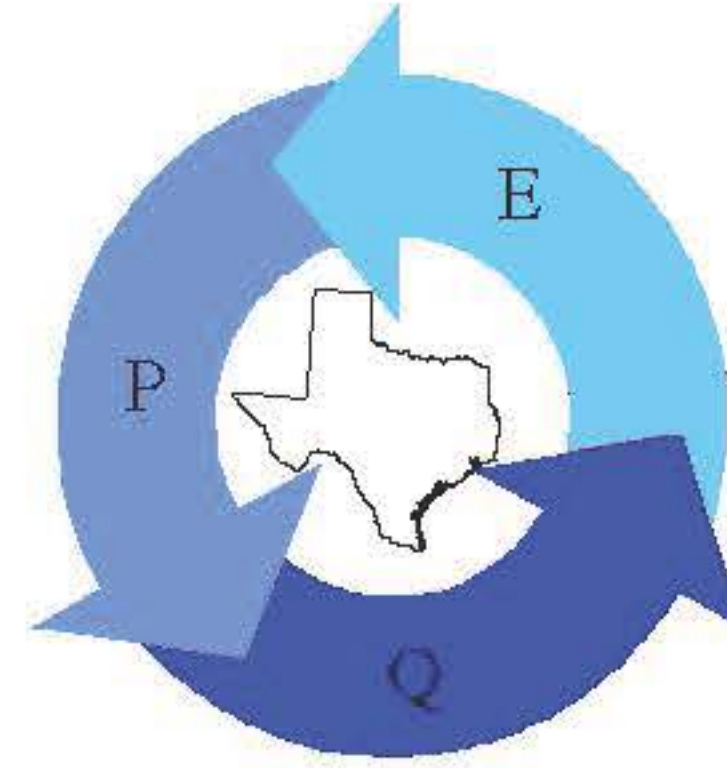


*Spatial Water Balance of Texas*

By Seann M. Reed, David R. Maidment, and Jérôme Patoux




---

**TABLE OF CONTENTS**

- ✦ [1. INTRODUCTION](#)
- ✦ [2. LITERATURE REVIEW](#)
  - [2.1 Atmospheric Water Balance Studies](#)
  - [2.2 Soil Water Balance Studies](#)
  - [2.3 Surface Water Balance Studies](#)
    - [2.3.1 Water Balances of Texas](#)
    - [2.3.2 Runoff Mapping](#)
- ✦ [3. ATMOSPHERIC WATER BALANCE](#)
  - [3.1 Atmospheric Data](#)
  - [3.2 Methodology](#)
    - [3.2.1 Water Balance Equations](#)
    - [3.2.2 A Control Volume over Texas](#)
    - [3.2.3 Direct Computation and Flux Integration Approaches to Estimate Divergence](#)
      - [3.2.3.1 Divergence approach](#)
      - [3.2.3.2 Flux integration approach](#)
  - [3.3 Results and Discussion](#)
    - [3.3.1 Results](#)
    - [3.3.2 Sources of error](#)
    - [3.3.3 Summary and Discussion](#)
- ✦ [4. SOIL-WATER BALANCE](#)
  - [4.1 Methodology](#)
    - [4.1.1 Model Description](#)
    - [4.1.2 Description of input data](#)
      - [4.1.2.1 Climate data](#)
      - [4.1.2.2 Water-holding capacity data](#)
      - [4.1.2.3 Open Water Evaporation Estimates](#)
      - [4.1.2.4 Radiation Data](#)
    - [4.1.3 Water-holding capacity of the soil](#)
    - [4.1.4 Estimating Actual Evapotranspiration](#)
    - [4.1.5 Budgeting soil moisture to yield surplus](#)
    - [4.1.6 Balancing Soil Moisture](#)
  - [4.2 Potential Evapotranspiration](#)
    - [4.2.1 Potential evaporation vs. potential evapotranspiration](#)
    - [4.2.2 Penman combination method](#)
    - [4.2.3 Simpler Methods](#)
      - [4.2.3.1 Pan coefficients](#)
      - [4.2.3.2 Priestley-Taylor Method](#)
      - [4.2.3.3 Comparison of Pan and Priestley-Taylor Methods](#)
  - [4.3 Results](#)
  - [4.4 Summary](#)
- ✦ [5. SURFACE WATER BALANCE](#)
  - [5.1 Overview](#)
  - [5.2 Methodology](#)
    - [5.2.1 Digital Elevation Model Processing](#)
    - [5.2.2 Selecting Gaging Stations for Analysis](#)
    - [5.2.3 Watershed Delineation](#)
    - [5.2.4 Compiling Watershed Attributes](#)
      - [5.2.4.1 Determining Mean Precipitation and Net Inflow](#)
      - [5.2.4.2 Reservoir Evaporation](#)
      - [5.2.4.3 Urban Land Use](#)
      - [5.2.4.4 Recharge](#)
      - [5.2.4.5 Springs](#)
  - [5.3 Results and Discussion](#)
    - [5.3.1 Expected Runoff](#)
    - [5.3.2 Mapping Actual Runoff and Evaporation](#)
    - [5.3.3 Mapping the Bowen Ratio](#)
    - [5.3.4 Summary Tables](#)
    - [5.3.5 Summary and Discussion](#)
- ✦ [6. CONCLUSIONS](#)
- ✦ [7. ACKNOWLEDGEMENT](#)
- ✦ [8. REFERENCES](#)
- ✦ [9. APPENDIX](#)

## 1. INTRODUCTION

Water availability is critical to the economy in the state of Texas. Numerous reservoirs and conveyance structures have been constructed across the State to meet the water supply needs of farmers, municipalities, industries, and power generating facilities. Despite this extensive water management system, water supply remains a concern because of increasing populations and uncertainties about climate stability. The rainfall map of Texas shown in Figure 1.1 clearly shows that water management is a spatial problem. The State as a whole receives about  $711 \text{ mm year}^{-1}$  of rainfall, while the area of the State east of the 100th meridian receives  $890 \text{ mm year}^{-1}$  and the area west of the 100th meridian receives only  $457 \text{ mm year}^{-1}$ . In addition to water supply concerns, the assessment of non-point source pollution is another important issue that is largely dependent on the spatial distribution of runoff. Although, the focus of this report is not to address water supply or pollution issues directly, an improved understanding of the spatial water balance the partitioning of precipitation between evaporation, runoff, and groundwater recharge at different points in space will directly benefit those who wish to assess water resource availability and non-point source pollution potential across the State.

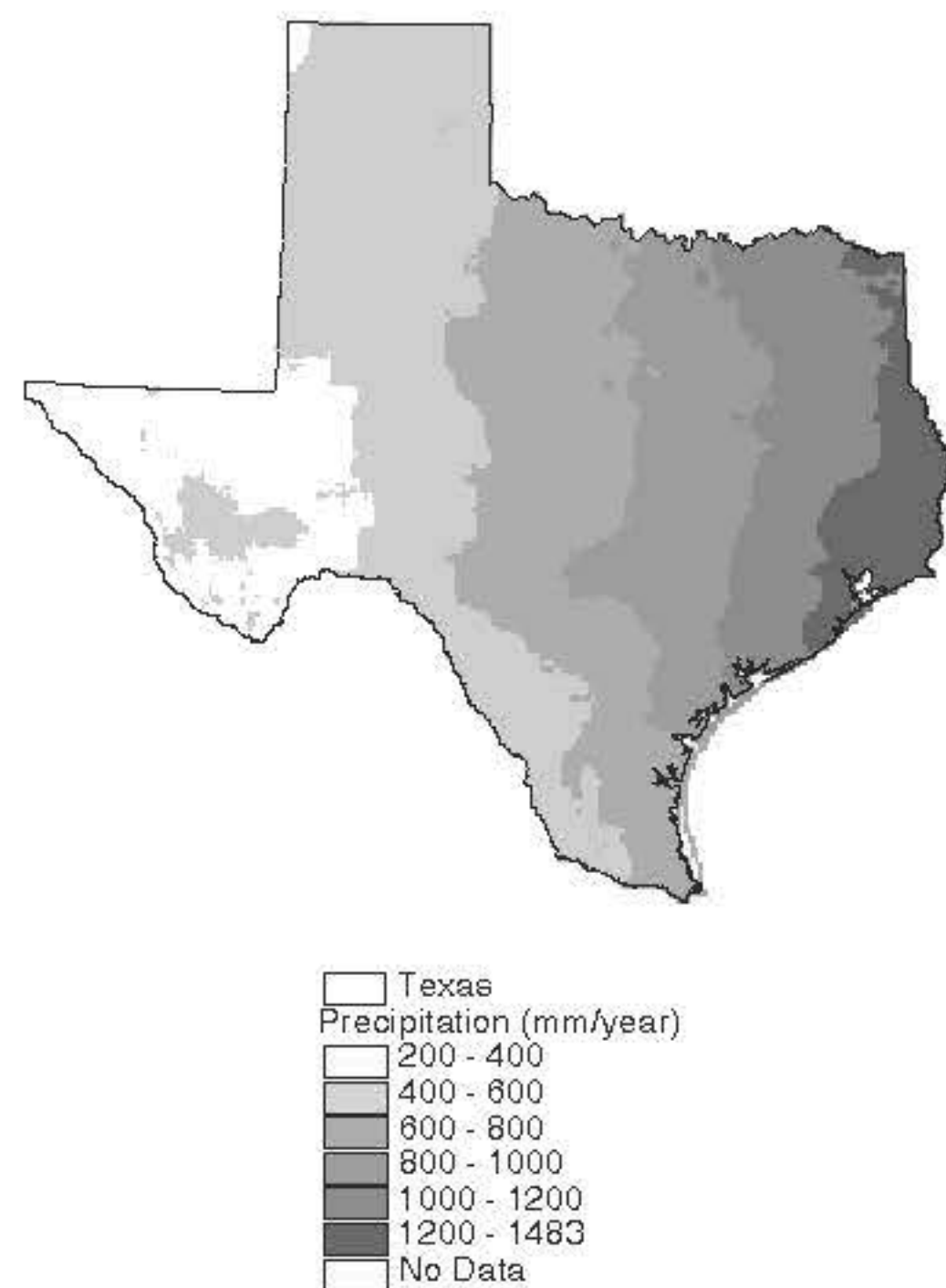


Figure 1-1: Mean Annual Rainfall in Texas from Oregon State PRISM Study (Daly, 1994)

The goal of this study was to gain an improved understanding of the stocks of water in different components (air, soil, water bodies) of the hydrologic cycle and the fluxes between these components. A basic approach for determining stocks and fluxes involves the calculation of a water balance. A water balance, applied to a particular control volume, is an application of the law of conservation of mass which states that matter cannot be created or destroyed. To achieve a balance, the rate of change of storage of water within the control volume must be equal to the difference between its rates of inflow and outflow across the control surface.

In this study, three independent water balance models were constructed to model different components of the hydrologic cycle an atmospheric water balance, a soil-water balance, and a surface water balance. These models were constructed using a geographic information system (GIS). A GIS provides a framework for storing and manipulating spatial data and facilitates modeling on control volumes of various sizes and shapes. In all three cases, the choice of modeling unit was driven by the resolution and characteristics of the input data. The control volumes for the atmospheric, soil, and surface water balance models respectively are (1) an imaginary column confined horizontally by the boundary of Texas and extending to the 300 mb pressure level, (2) 0.5 cells with a depth equal to the plant-extractable water capacity of the soil, and (3) 166 gaged watersheds of differing sizes and shapes. Neither the atmospheric nor the surface water balance involve any simulation of physical processes and are simply mass balances based on empirical data. The soil-water balance does attempt to simulate evaporation from the soil through the use of a soil-moisture extraction function. Both the atmospheric and soil-water balance models are time-varying models, while the surface water balance model is steady-state and uses an empirical relationship to estimate mean annual runoff and evaporation in ungaged areas. One advantage of making three independent water balance calculations is that checks for consistency can be made among the three models. For example, all three models yield an estimate of *actual* evapotranspiration which is a difficult quantity to estimate, particularly at the regional scale. Previous studies at the scale of Texas have estimated only evaporation from open water surfaces and *potential* evapotranspiration from the land surface (TDWR, 1983; Dugas and Ainsworth, 1983).

Of the three methods, the surface water balance has the least uncertainty and the greatest spatial resolution. Current atmospheric data do not seem to support accurate calculations of net moisture influx at the scale of Texas on a monthly time scale as attempted in this study. The soil-water balance method employed here is limited by the use of monthly data and its overly simplified representation of land surface hydrology. Despite their weaknesses, the atmospheric and soil-water balance methods do provide information and insights that cannot be gleaned from the surface water balance alone.

In terms of usable runoff maps for engineering and planning, the surface water balance provides the best results. The surface water balance yields gage-calibrated maps of mean annual runoff and evaporation for the entire state on a 500 m grid. To estimate runoff in ungaged areas, a scale independent "expected" rainfall-runoff curve was developed. This rainfall-runoff curve represents runoff that would be expected in the absence of large amounts of reservoir evaporation, urbanization, and recharge-springflow activity. Maps of actual runoff and expected runoff were created for the entire state. A map of the differences between actual and expected runoff shows where human activities strongly influence runoff in Texas. By combining runoff information with the topographic information in a 500 m digital elevation model, accumulated flow maps were created and these maps show statewide spatial trends such as the increased density of stream networks in East Texas, while also capturing localized phenomena such as large springflows and agricultural diversions. The maps are presented in this report in paper form and the data used to create these maps can be obtained in digital form as Arc/Info grids on CD-ROM from the Center for Research in Water Resources, University of Texas at Austin.

## 2.0 LITERATURE REVIEW

### 2.1 Atmospheric Water Balance Studies

A number of researchers have used the atmospheric water balance to estimate hydrologic fluxes. Among these researchers, Rasmusson, 1967, Brubaker *et al.*, 1994, and Oki *et al.*, 1995, describe atmospheric water balance studies at river basin, continental, and global scales. Rasmusson, 1967, analyzes the characteristics of total water vapor flux fields over North America and the Central American Sea. A noteworthy observation made by Rasmusson is that a large diurnal wind system covering the central United States, part of Mexico, and the Central American Sea produces significant diurnal variations in the transport of water vapor. By decomposing the vertically integrated vapor flux term into mean motion and transient eddy terms, where the mean motion term is at a time scale of one month and the transient eddy term describes motion at a time scale of less than one month, Brubaker *et. al.* also observe important vapor flux transport at sub-monthly time scales. Brubaker *et. al.* note that poleward eddy flux transport from the Gulf of Mexico is significant, particularly during the winter months. From these observations, Brubaker *et. al.* surmise that the use of monthly-averaged or sparse data may significantly underestimate the eddy flux component of vapor transport. These observations are relevant to the interpretation of our results, as discussed in Section 3.3. Brubaker *et al.* also note that the accuracy of runoff estimates made using atmospheric data increases with the size of the study area and cite a recommendation by Rasmusson, 1977, that a minimum area of  $10^6$  km<sup>2</sup> should be used. The area of Texas is about  $0.7 \times 10^6$  km<sup>2</sup>. Improvements in observational networks and general circulation models may justify runoff estimation on smaller areas in the future.

If the annual change in atmospheric water storage and surface water storage are both negligible, runoff estimates can be obtained from the vertically integrated vapor flux convergence ( $-\nabla \cdot \vec{Q}$ ). Using four years of data from the European Centre for Medium-Range Weather Forecasts (1985-1988), Oki *et al.* compared convergence values with the observed annual runoff for 70 river basins throughout the world. Differences between vapor flux convergence and measured runoff varied widely, although larger river basins tended to show smaller differences. On average, the vapor flux convergence was about 2/3 of the measured runoff. Oki *et al.* also made a more detailed study of the Chao Phraya River basin in Thailand which drains 178,000 km<sup>2</sup>. Oki *et al.* estimated annual runoff, monthly evaporation, and monthly storage for the Chao Phraya from 1985 to 1988. The evaporation and river basin storage values were estimated by augmenting atmospheric data with precipitation and runoff data. In the Chao Phraya basin, the vapor flux convergence was consistently higher than observed runoff; however, the temporal variations of vapor flux convergence and runoff were comparable. This was illustrated by applying a reduction factor to the convergence values.

Significant uncertainties in runoff estimation using atmospheric data still exist even at the continental scale. Both Brubaker *et al.* and Oki *et. al.* compare their continental runoff estimates with those given by Baumgartner and Reichel, 1975, for river runoff. For North America, Brubaker *et. al.* estimate annual runoff as 84.6 mm/year while Oki *et. al.* estimate 263 mm/year and Baumgartner and Reichel give 223 mm/year. Both Brubaker *et al.* and Oki *et al.* make note of the fact that poorly defined continental or basin boundaries may contribute to inaccuracies in runoff estimation. This problem is solved in the current study of Texas by using a geographic information system in which any arbitrarily defined boundary can be used to compute the water balance, although the problem remains that atmospheric soundings are sparse remains.

### 2.2 Soil Water Balance Studies

Where detailed data about soil layers, depth to groundwater, and vegetation are not available, hydrologists have often resorted to simple bucket models and budgeting schemes to model near-surface hydrology. Despite numerous uncertainties associated with the simple soil-water budget model like the one used in this study, many researchers have applied this type of model to problems ranging from catchment scale studies to the global water balance and climate change scenarios (Thornthwaite, 1948; Shiklomanov, 1983; Manabe, 1969; Mather, 1978; Alley, 1984; Willmott *et al.*, 1985; Mintz and Walker, 1993; Mintz and Serafini, 1992). This approach is attractive because of its simplicity. The simple "bucket" model used here requires minimal input data: precipitation, potential evapotranspiration, and soil-water holding capacity. The studies by Willmott *et al.*, Mintz and Walker, and Mintz and Serafini, are climatology studies that present the global distributions of precipitation, evapotranspiration, and soil moisture. Mintz and Serafini compare their evapotranspiration estimates for sixteen major river basins throughout the world with those derived from river runoff analysis made by Baumgartner and Reichel, 1975, and the values show reasonable agreement.

At a smaller scale, Mather, 1978, (Chapter 4) describes the application of a soil-water budget model to several watersheds in the coastal plains of Delaware, Maryland, and Virginia. Comparisons between measured and computed runoff values are rather poor for monthly data, but better for annual data, although Mather suggests further refinement of the method even for annual values. In its simplest form, the soil-water budget model does not account for situations where the precipitation rate is greater than the infiltration capacity of the soil. Mather describes one approach to remedy this problem, that is, to first use the SCS method to estimate direct overland runoff and subtract this amount from the precipitation before it is allowed to enter the soil "bucket." This approach appears to yield better results (Mather, Chapter 4). A similar approach of taking an initial rainfall abstraction before allowing precipitation to enter the soil column for climatological budgeting was used in a study of the Niger Basin described by Maidment *et al.*, 1996 (further description available at <http://www.ce.utexas.edu/prof/maidment/gishydro/africa/africa.htm>). In the Niger Basin study, the surplus from the soil-water budget is passed to a surface and groundwater routing model which is in turn calibrated with observed runoff.

### 2.3 Surface Water Balance Studies

#### 2.3.1 Water Balances of Texas

The surface water balance, a commonly used method in hydrologic studies, relies on the fact that with the exception of coastal areas, the landscape can often be divided into watershed units from which there is only one surface water outflow point. Provided that the average watershed precipitation and runoff can be measured with reasonable accuracy, the annual evaporative losses from a watershed can be estimated. Of course this assumes that change in storage is negligible and that there are no significant inter-watershed transfers via groundwater or man-made conveyance structures. Empirical relationships are often used to estimate mean annual or mean monthly flows in ungaged areas; this approach is used in this study.

Two water balance studies that are particularly relevant to Texas are those by Ward, 1993, and the Texas Board of Water Engineers, 1961. Ward presents a water balance similar to that described here in which he estimates precipitation, evapotranspiration, runoff, recharge, and water demands for four different hydroclimatological regions in Texas and for the State as a whole. To estimate annual runoff, Ward uses an empirical relationship between rainfall and runoff. A similar approach is used in this study, although the rainfall-runoff relationship derived here is used in conjunction with a large database of measured values to develop spatially distributed maps of runoff. The Texas Board of Water Engineers (TBWE; now Texas Water Development Board) Bulletin 6001 is a study of surface runoff (1940-1956) from the major basins and sub-basins in Texas that uses measured flow data. To estimate runoff in ungaged watersheds or watersheds with insufficient streamflow records, the authors of Bulletin 6001 used a proportion of the observed runoff in a watershed with similar characteristics and an additional factor to account for the difference in precipitation if necessary. One product of Bulletin 6001 is a map of Texas sub-basins with printed values of runoff. Improvements in computer technology since 1961 allow for more detailed electronic maps to be generated in this study, although the idea of mapping runoff values is similar.

#### 2.3.2 Runoff Mapping

Three recently published articles by Arnell, 1995; Lullwitz and Helbig, 1995; and Church *et al.*, 1995, describe studies of runoff mapping. All three use a geographic information system (GIS) to manage spatial data at a regional or continental scale. The paper by Arnell summarizes five approaches for deriving gridded runoff maps at a 0.5 grid resolution including (1) simply averaging the runoff from all stations within each grid cell, (2) statistically interpolating runoff between gages, (3) using an empirical relationship that relates runoff to precipitation, potential evaporation, and temperature, (4) using a soil-water balance type model, and (5) overlaying grid cells onto catchment runoff maps to derive area-weighted runoff estimates. Arnell evaluates all but method (4) by mapping runoff onto 0.5 grid cells over a large portion of western Europe, and then intersecting the results with seven gaged river basins to validate the results. The results show that method (5) produces the most reasonable estimates. In a study similar to that of Arnell, Lullwitz and Helbig created 0.5 runoff maps for the Weser River in Germany. Both Arnell and Lullwitz and Helbig note that 0.5 runoff maps can be useful for validating general circulation models (GCM's). Church *et. al.* present maps of evapotranspiration (ET) and runoff/precipitation (R/P) ratios for the northeastern United States. Church *et. al.* use an interpolation method to create runoff maps. Church *et al.* found their results to be useful in assessing the effects of acidic deposition.

The approach used for runoff mapping in this study is different than any of the methods described above, although it is most similar to Arnell's method 5. The approach taken here combines an empirical rainfall-runoff relationship and watershed runoff balancing.

3.1 Atmospheric Data  
 Two sources of atmospheric data were used in this study. One data set was provided by Allen Bradley at the University of Iowa Institute for Hydraulic Research and the other by the National Meteorological Center (NMC). The data provided by Bradley originate from rawinsonde soundings. These rawinsondes are launched twice daily (0 and 12 Coordinated Universal Time (UTC)) to measure temperature, humidity, and wind profiles at several levels in the atmosphere. Using these data, Bradley estimated the specific humidity at each measurement level and used the following equations to estimate the vertically integrated vapor flux:

$$Q_v = \frac{1}{g} \int_{p_0}^{p_1} q \omega dp \quad (3.1a)$$

$$Q_w = \frac{1}{g} \int_{p_0}^{p_1} \omega v dp \quad (3.1b)$$

In these equations,  $Q_v$  is the zonal (east-west) component of vapor flux in  $[kg \cdot m^{-1} \cdot s^{-1}]$ ,  $Q_w$  is the meridional (north-south) component of vapor flux in  $[kg \cdot m^{-1} \cdot s^{-1}]$ ,  $q$  is the specific humidity  $[g \cdot m^{-3}]$ ,  $u$  is the zonal component of wind velocity  $[m \cdot s^{-1}]$ ,  $v$  is the meridional component of wind velocity  $[m \cdot s^{-1}]$ ,  $p$  is the pressure  $[Pa]$ , and  $g$  is the gravitational constant  $[9.81 \cdot m \cdot s^{-2}]$ . The negative sign arises due to the fact that the hydrostatic assumption was used to convert from elevation to pressure. The limits of integration are the surface pressure ( $p_0$ ) and the pressure at the top of the atmosphere ( $p_1$ ). Strictly speaking, the top of the atmosphere does not exist since there is no physical boundary constraining the atmosphere below a certain level; however, the transport of water vapor across the 300 mb (30.3 kPa) level is considered negligible so 300 mb was defined as the top of the atmosphere in these computations.

Bradley provided mean monthly integrated vapor flux values for October 1972 to December 1994. The mean monthly values for 0 and 12 Coordinated Universal Time were provided separately. These two values were averaged to estimate mean monthly flux. The data files from Bradley were provided in two formats: integrated flux estimates interpolated to a 2 grid using a standard meteorological method for interpolation called the Barnes objective analysis, and flux estimates interpolated to points on the Texas border using bilinear interpolation. These two data formats facilitate computing the two atmospheric water balance using either a divergence approach or a flux integration approach as described below. Computations were made using both approaches as a check, and the two methods yielded consistent results.

Another data set, containing monthly atmospheric moisture divergence estimates on a 2.5 grid, was obtained from the National Meteorological Center (NMC) for the 26 month period from June 1991 to July 1993. At NMC, a general circulation model (GCM) is run two to four times per day to predict atmospheric conditions a few hours in advance. After these few hours have passed, observational data including rawinsonde data, satellite temperature and moisture data, and surface observations, are used to adjust the predictions and the next simulation is run. A general circulation model fills gaps in regions with sparse observations and creates atmospheric data sets on regular grids. The NMC monthly divergence estimates used in this study are outputs from the general circulation model. These values are the results of a simulation only and were not modified after the fact to fit actual measurements (Patoux, 1994). No computations were required to determine the divergence on the NMC grid because these values were provided; therefore, the calculations described below refer only to the Bradley data.

3.2 Methodology  
 3.2.1 Water Balance Equations

The mass conservation equation for water vapor in the atmosphere can be written as

$$\frac{\partial W}{\partial t} - \nabla \cdot \vec{Q} + E - P \quad (3.2)$$

where  $W$  is the amount of water vapor stored in the atmospheric column,  $\nabla \cdot \vec{Q}$  is the divergence or net outflow of water vapor across the sides of the atmospheric column,  $Q$  is the vapor flux,  $E$  is evaporation, and  $P$  is precipitation. The quantity  $W$  is also referred to as the precipitable water and may be expressed in terms of mean air unit surface area ( $[M \cdot L^{-2}]$ ) or converted to an equivalent depth of liquid water ( $1000 \text{ kg} \cdot m^{-2}$ ). The divergence is represented mathematically by  $\nabla \cdot \vec{Q} = \frac{\partial Q_x}{\partial x} + \frac{\partial Q_y}{\partial y}$  and measures the difference between inflow and outflow to a region. A positive divergence means that outflow is greater than inflow, and a negative divergence (or convergence) means that inflow is greater than outflow. The units of divergence are  $[M \cdot L^{-2} \cdot T^{-1}]$  but may also be expressed as depth of liquid water per time  $[L \cdot T^{-1}]$  results in these units. To show how the atmospheric water balance can be used to estimate the runoff from a river basin, a similar equation can be written for the surface water balance.

$$\frac{\partial H}{\partial t} = R_{in} - R_{out} - E + P \quad (3.3)$$

In Equation 3.3,  $H$  is the depth of liquid water storage in the basin,  $R_{in}$  and  $R_{out}$  are the inflow and outflow of surface or subsurface runoff,  $E$  is evaporation, and  $P$  is precipitation. Combining Equations 3.2 and 3.3 yields the expression:

$$-\nabla \cdot \vec{Q} - \nabla \cdot \vec{Q}_s = \frac{\partial H}{\partial t} (R_{in} - R_{out}) = P - E \quad (3.4)$$

In mean annual water balance computations, the change in atmospheric storage ( $\frac{\partial W}{\partial t}$ ) and surface water storage ( $\frac{\partial H}{\partial t}$ ) are often assumed to be negligible so that the negative of the divergence provides an estimate of runoff.

$$-\nabla \cdot \vec{Q} = R_{out} - R_{in} = P - E \quad (3.5)$$

It is seen in Equation 3.5 that if the divergence ( $\nabla \cdot \vec{Q}$ ) in a region is positive, then evaporation is greater than precipitation ( $P < E$ ), while a negative divergence or 'convergence' indicates that precipitation is greater than evaporation ( $P > E$ ). One goal of this study was to estimate the divergence or net influx of water to the atmosphere above Texas.

3.2.2 Control Volume over Texas

To define an atmospheric column for vapor flux calculations, the boundary of Texas was generalized by dividing it into straight segments, each with a length of approximately 100 km, and this boundary was extended vertically to the top (200 mb level) of the atmosphere. In visualizing this control volume, it is important to keep in mind that the height of the atmosphere (10-15 km) is thin compared to the horizontal extent of Texas. Figure 3-1 shows that only 42 cells are required to cover the state of Texas and surrounding areas, while Figure 3.2 shows the thickness of the atmosphere relative to the horizontal extent of a 2 grid cell.



Figure 3-1: 2 Degree Cells Overlaid on the Texas Border  
 Figure 3-2: Dimensions of a 2 Degree Atmospheric Column in South Texas

3.2.3 Direct Computation and Flux Integration Approaches to Estimate Divergence  
 3.2.3.1 Divergence approach

Two methods for computing divergence ( $\nabla \cdot \vec{Q}$ ) were applied to the Bradley data set and, as expected, both methods gave consistent results. In the first method, the divergence was computed directly from the 2 grid by using a finite difference approximation to the divergence equation in spherical coordinates. Equation 3.4 gives an expression for divergence in both Cartesian and spherical coordinates.

$$\nabla \cdot \vec{Q} = \frac{\partial Q_x}{\partial x} + \frac{\partial Q_y}{\partial y} \quad (3.6a)$$

$$\nabla \cdot \vec{Q} = \frac{1}{R_e \cos \phi} \left( \frac{\partial Q_\lambda \cos \phi}{\partial \lambda} + \frac{\partial Q_\phi}{\partial \phi} \right) \quad (3.6b)$$

$R_e$  is the radius of the model earth taken as 6371.2 km,  $Q_\lambda$  and  $Q_\phi$  are the zonal and meridional components of vapor flux (previously denoted as  $Q_x$  and  $Q_y$  respectively),  $\lambda$  is longitude in radians, and  $\phi$  is latitude in radians. The spherical form of the divergence equation can be derived following the methodology given by Kravitz, 1993, Section 8.12. The following centered difference approximation was used to calculate divergence directly from the 2 gridded data.

$$\nabla \cdot \vec{Q}(\phi, \lambda) = \frac{1}{R_e \cos(\phi)} \left( \frac{Q_{\lambda(\lambda+\Delta\lambda)} - Q_{\lambda(\lambda-\Delta\lambda)}}{(\lambda_{i+1} - \lambda_{i-1})} + \frac{\cos(\phi_{\phi+\Delta\phi})Q_{\phi(\phi+\Delta\phi)} - \cos(\phi_{\phi-\Delta\phi})Q_{\phi(\phi-\Delta\phi)}}{(\phi_{i+1} - \phi_{i-1})} \right) \quad (3.7)$$

The  $10 \times 9$  computational mesh used for the Bradley data is shown in Figure 3-3. For points on this mesh in columns 1 and 10 ( $i = 1$  and 10), Equation 3.7 was modified to use a forward or backward difference approximation as appropriate, because data values outside of this mesh were not provided. The use of a forward or backward difference approximation did not affect any of the cells intersecting the boundary of Texas.

The units of the divergence computed with Equation 3.7 are  $[kg \cdot m^{-1} \cdot s^{-1}]$ . To estimate the net influx in the atmosphere above Texas, cells centered on the mesh points depicted in Figure 3.3 were intersected with the Texas boundary as shown in Figure 3.4. The boundary of Texas shown in Figure 3.4 is the same generalized boundary use in the flux integration calculations described in the next section. Intersection is a GIS term that describes an overlaying of two spatial data sets. In this case, the border of Texas was intersected with the 2 cell layout of atmospheric data to determine the area of each cell lying within the State. By summing up the divergence estimates and using these included areas as weights, an estimate of the divergence for the State as a whole was made. This intersection was made in a projected plane; the projection used was an Albers equal-area projection.

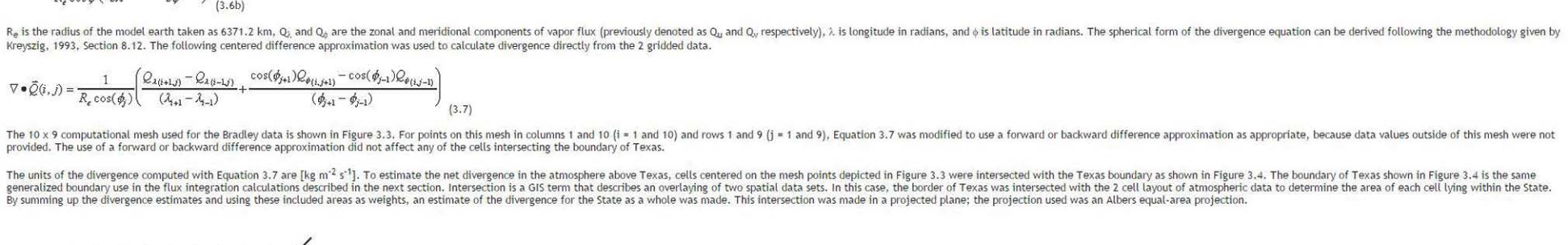


Figure 3-3: Computational Mesh for Divergence Calculations  
 Figure 3-4: Computational Cells Intersected with the Generalized Boundary of Texas

3.2.3.2 Flux integration approach

Thanks to the divergence theorem of Gauss (Kravitz, 1993, p. 545, 551), an alternative method for calculating divergence is available that involves calculating the moisture flux across line segments that make up the Texas border. This approach is interesting because the flux across any arbitrary boundary line can be estimated. Because a three dimensional problem was reduced to a two dimensional problem through vertical integration of the vapor flux, the divergence theorem in two dimensions can be applied:

$$\nabla \cdot \vec{Q} = \frac{1}{A} \oint \vec{Q} \cdot \vec{n} dl \quad (3.8)$$

Rather than using a vector dot-product as in Equation 3.8, the right hand side of this equation can be evaluated by applying a vector cross-product to each border segment and summing the result for each to determine the net flux into the Texas atmosphere. This concept is illustrated in Figure 3-5.



Figure 3-5: Vector Cross Product

The vector  $\vec{n} = (n_x, n_y)$  defines the boundary line where  $x$  is in the direction of parallels of latitude and  $y$  is in the direction of meridians of longitude. As before, the vector  $Q = (Q_x, Q_y)$  is the atmospheric moisture flux in  $[kg \cdot m^{-1} \cdot s^{-1}]$  where  $Q_x$  is in the  $x$  direction and  $Q_y$  is in the  $y$  direction. The mass flow rate across a boundary segment in  $[kg \cdot s^{-1}]$  can be obtained from the vector cross-product as follows:

$$\vec{Q} \cdot \vec{n} = Q_x n_x + Q_y n_y \quad (3.9)$$

In this problem, the boundary segments that make up the border of Texas are defined so that they all point in a clockwise direction, the interior of the region is to the right of each boundary vector and the exterior is to the left. The result of the vector cross product is a vector oriented in the vertical direction. If this vector is positive, this indicates mass leaving the region and if this vector is negative, this indicates mass entering the region. For net flux calculations, only the magnitude of the resulting vector  $\vec{Q} \cdot \vec{n}$  is needed. The total outflow is determined by summing the magnitudes of all  $\vec{Q} \cdot \vec{n}$  vectors pointing in the positive  $\vec{K}$  direction and the total inflow by summing the magnitudes of all  $\vec{Q} \cdot \vec{n}$  vectors pointing in the negative  $\vec{K}$  direction. The net flux or divergence is outflow minus inflow.

In this calculation, the direction of the vector flux components are defined in geographic space and the geometric relationship between the flux vectors and border segments is also determined in geographic space; however, the lengths of the border components ( $|L_x|$  and  $|L_y|$ ) correspond to the length of these segments as measured along the surface of the earth. To estimate  $|L_x|$  and  $|L_y|$  given the latitude and longitude of segment endpoints, the length of a radian of longitude and a radian of latitude on the earth's surface (with the earth represented as an ellipsoid) were multiplied by the difference between the longitude and latitude of the two segment endpoints as follows:

$$|L_x| = \frac{a \cos \phi}{(1 - e^2 \sin^2 \phi)^{1/2}} \Delta \lambda \quad (3.10a)$$

$$|L_y| = \frac{a(1 - e^2)}{(1 - e^2 \sin^2 \phi)^{3/2}} \Delta \phi \quad (3.10b)$$

The equations for the length of a radian along a meridian of longitude and the length along a parallel of latitude were taken from Snyder, 1987, p. 25. The parameters for the Clarke 1866 ellipsoid were used to evaluate Equation 3.10 because this was the ellipsoid used to define the Texas border; in Equation 3.10,  $a$  is the radius of curvature for the ellipse in the plane of the Equator ( $a = 6378206.4 \text{ m}$ ),  $e$  is the eccentricity ( $e = 0.00045815$ ),  $\Delta \lambda$  is the longitudinal difference between segment end points [radians], and  $\Delta \phi$  is the latitudinal difference between segment end points [radians].

3.3 Results and Discussion  
 3.3.1 Results

Figure 3.6 shows the results of the monthly divergence calculations for 1973 to 1994 using the Bradley data. The chart of Figure 3.6 shows the results of direct divergence calculation on a spherical grid (Section 3.2.3.1). Although not shown here, the flux integration results (Section 3.2.3.2) are nearly identical (within 2% on average) as expected. Figure 3.7 presents the same data of Figure 3.6 averaged by year. Figure 3.8 provides a comparison of Bradley and NMC divergence for the 26 month period when the NMC data were available (June 1991 - July 1993). There are significant differences between these two estimates, both in variation of divergence throughout the year and the average divergence magnitudes. Assuming that the mean annual change in atmospheric storage is negligible, the 22 year average runoff ( $P-E$ ) from the Bradley data is 1206 mm year<sup>-1</sup> and the 2 year average runoff predicted from the NMC data is 379 mm year<sup>-1</sup>. Both of these estimates are much higher than observed surface runoff! A 30 year mean annual runoff of 78.4 mm year<sup>-1</sup> was estimated from the surface water balance described in Section 5 below. Such large errors in predicting runoff using the atmospheric water balance are not uncharacteristic for this type of study. Although Oki et al. find good agreement between convergence and observed runoff for several basins in the analysis of 70 basins worldwide, they also report a wide range of errors in which the vapor flux convergence may be up to 80 times the observed runoff or the vapor flux convergence may predict a net evaporation 28 times greater than observed runoff. Several sources of error in making atmospheric flux calculations are discussed in Section 3.3.2.

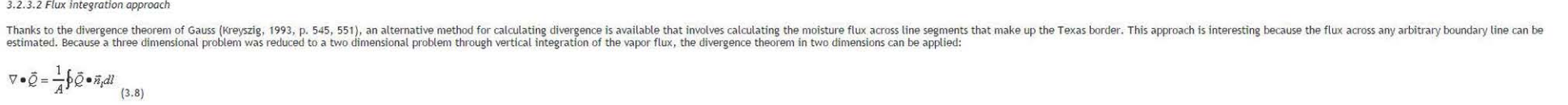


Figure 3-6: Monthly Divergence of Water Vapor Over Texas for 22 Years

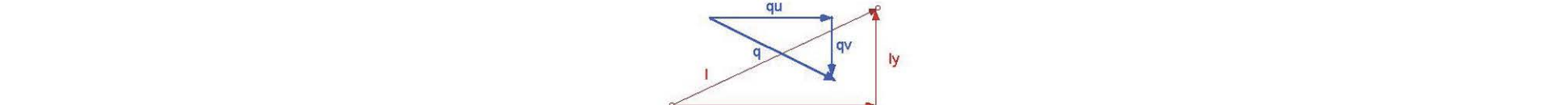


Figure 3-7: Yearly Mean Divergence of Water Vapor Over Texas (1973 - 1994)

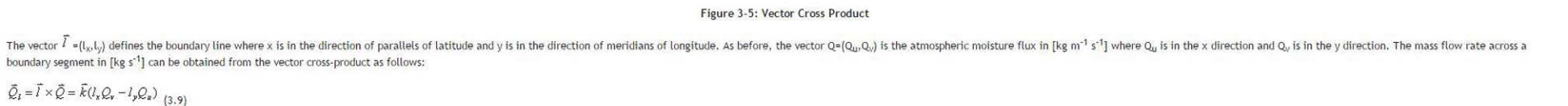


Figure 3-8: Net Influx of Water to the Atmosphere Above Texas, June 1991 - July 1993

If it is assumed that the change in storage from month to month in the atmosphere is negligible, an evaporation estimate can be made as  $(E = \nabla \cdot \vec{Q} + P)$ . Taking statewide average monthly precipitation estimates for 1992 from the study of Patoux, 1994 (Figure 4.2.7), rough monthly evaporation estimates are shown in Figure 3.9 and compared to the Bradley and NMC data respectively. The average precipitation for Texas were made using Thiessen polygon gauges from the locations of precipitation stations and computing the area average using an intersection procedure similar to that described in Section 3.2.1. Clearly the evaporation estimates shown in Figure 3.9 are unreasonable because negative evaporation estimates don't have physical meaning. Using the Bradley data, the total  $\nabla \cdot \vec{Q}$  for 1992 is -310 mm,  $P$  for 1992 is 840 mm, giving  $E_{1992} = 530 \text{ mm}$  if the annual change in storage is negligible. Figure 3.10 shows more reasonable monthly evaporation estimates; however, the annual divergence estimate (-309 mm) is still quite high relative to annual runoff and changes in atmospheric storage may not be an adequate explanation for the relatively large negative evaporation estimates in January, February, and March.



Figure 3-9: Evaporation Estimates from Bradley Divergence + Precipitation in 1992

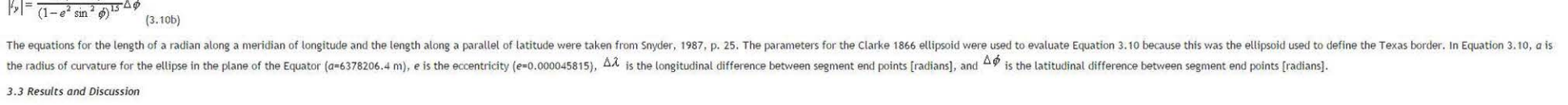


Figure 3-10: Evaporation Estimates from NMC Divergence + Precipitation

Unfortunately, very little data on atmospheric storage was available for this study. In unpublished follow up work to the study by Patoux, 1994, Patoux estimated the moisture content of the atmosphere over Texas for the first 6 months of 1991. The moisture content increased from about 17.1 mm in January to 54.7 mm in June, with increases of 3.6 mm, 2.4 mm, 3.4 mm, 7.8 mm, and 20.4 mm in the intervening months. This information shows that the atmosphere holds more moisture in the warm summer months. It doesn't appear that large discrepancies illustrated in Figures 3.9 and 3.10 can be explained by these relatively modest atmospheric moisture changes.

In addition to making net flux calculations, a simple program for displaying flux vectors in a geographic information system was developed for use in this study. Looking at the flux vectors gives a sense of where moisture enters and leaves the State, and also gives a feel for seasonal and annual trends in moisture flux magnitudes. Figures 3.11 and 3.12 show moisture flux vectors for January and July 1973. The moisture flow over Texas drastically increased during the Midwest flood of 1993 which is shown in Figure 3.13. Comparing Figures 3.12 and 3.13 shows the difference in summer moisture flux between 1973 and 1993.

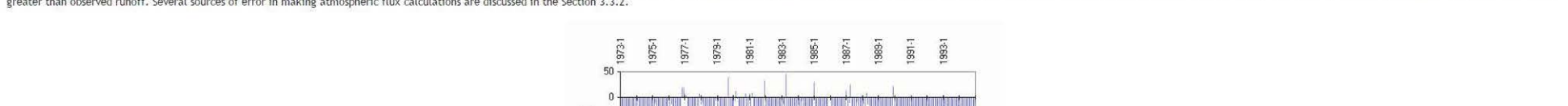


Figure 3-11: Moisture Flux Vectors in January, 1973



Figure 3-12: Moisture Flux Vectors in July, 1973



Figure 3-13: Moisture Flux Vectors in July, 1993

3.3.2 Sources of error

The sparseness of observation points, both horizontally and vertically, leaves room for significant error in the atmospheric flux calculations. Even if estimates at all the 2 grid points were accurate, this leaves only about 42 observations. After vertical integration, to describe the flux over an area of 690,000 km<sup>2</sup>, in addition to problems with sparseness of measurements in the horizontal direction, Brubaker et al. note that the vertical resolution of atmospheric soundings, which typically include measurements at about 6 levels from 1000 to 300 mb (about 0 - 10 km), do not adequately resolve the atmospheric boundary layer (for which a typical depth is 1 km) where a large fraction of the atmospheric water vapor can be found.

Because of the large magnitudes of the numbers under consideration, a small error in the estimate of vapor flux across a single line segment may have a relatively large impact on the net influx computation. For example, the flux across segment 1 (86 km) in Figure 3.11 is  $9.180 \times 10^6 \text{ kg} \cdot \text{s}^{-1}$  which is equivalent to about 880 m<sup>3</sup> s<sup>-1</sup> or 36 mm month<sup>-1</sup> when dividing by the area of the region being considered this value is significant when compared with the evaporation estimates given in Table 3.1 below. The fact that there are large volumes of water both entering and leaving the State means that calculating the net influx requires taking the vertically integrated moisture flux into mean motion and transient eddy terms. They note that from a global perspective mean motion dominates  $Q_v$  while mean and transient eddy terms are of comparable magnitude in  $Q_w$ . From the results of their study, Brubaker et al. concluded that eddy flux terms contribute significantly to the north-south transport of water vapor, particularly along the Gulf of Mexico in the winter months. Thus, fluctuations on a few day time scale are important when considering the transport of water vapor, a conclusion also reached by Rasmusson, 1967.

3.3.3 Summary and Discussion

Two consistent methods for computing the divergence of atmospheric moisture using rawinsonde data have been described: one using a finite difference approximation on a spherical grid and one by summing fluxes across boundary lines. The results of these computations were compared with output from a general circulation model. In general, computations based strictly on observed data yielded poorer estimates of divergence, with the estimate of average annual divergence over Texas being 15 times greater than observed runoff. The divergence estimate from the general circulation model was about 5 times greater than observed runoff. Reasons for errors may include (1) the sparseness of observations, (2) errors associated with taking differences between large numbers, and (3) using monthly average flux values. With regard to the first reason for errors, improved observation networks and remote sensing may help to alleviate problems with data resolution in future studies. The United States National Meteorological Center is presently implementing a new mesoscale general circulation model over North America called the Eta model, using 40 km computational cells which will provide about 25 times greater horizontal resolution than the grid used in this study. The second problem may be difficult to overcome considering the large amounts of moisture that flow through the atmosphere relative to the amounts of precipitation, evaporation, and runoff. Statewide average estimates from this study indicate that the average annual throughflux (1973 - 1994) of atmospheric moisture is 7788 mm while the annual precipitation is 120 mm and average annual runoff is 78.4 mm (See Section 5). Indicating that only 9% of the moisture passing over the State falls as precipitation and 11% of this precipitation becomes runoff. With regard to the third problem, data for making calculations on shorter than monthly time steps are available, but were not used due to time and logistical constraints in this study.

When calculations made in this study were compared with the output of a National Meteorological Center GCM, the GCM results seemed more reasonable, but not entirely satisfactory. The GCM considers transient eddy behavior that is not captured by mean monthly observations because a much smaller time step is used. Simulation models also offer the advantage that equations of motion can be used to fill in areas with sparse observations. As products from higher resolution GCM simulations become available, simple operations in GIS can be used to estimate net fluxes into arbitrarily defined regions as done in this study.

Some additional information would have been useful to help assess the relative importance of different sources of error in this study. The use of 12 hourly data could have shed more light on problems associated with using monthly average values. It also would have been interesting to know the locations where rawinsonde observations were actually made. In addition, more water content computations could have been made to yield better evaporation estimates.

Table 3-1: Comparison of Bradley Data and Throughflux in 1977

Month	Influx (mm)	Outflux (mm)	Netflux (mm)	Throughflux (mm)	Throughflux/Netflux
1977-1	666.0	666.7	3.8	666.9	178
1977-2	416.2	419.7	3.4	418.0	122
1977-3	926.3	967.2	40.9	997.8	15
1977-4	624.2	545.2	79.0	552.2	7
1977-5	726.4	119.7	139.7	355.2	6
1977-6	938.1	618.9	-139.4	678.6	6.7
1977-7	715.0	494.6	-120.4	654.8	5.4
1977-8	819.5	577.7	241.9	696.6	2.9
1977-9	923.4	405.1	123.3	541.7	4.4
1977-10	603.0	545.6	57.5	574.3	11.0
1977-11	500.3	471.9	28.4	486.1	17.1
1977-12	737.4	5.0	734.8	145	

If there is a 10% error in the influx estimate for January 1977, then the true influx might be 731.5  $[mm \cdot month^{-1}]$ , making the netflux -42.8  $[mm \cdot month^{-1}]$  rather than 3.8  $[mm \cdot month^{-1}]$  which is a 1750% difference. The absolute value of the throughflux to netflux ratio is shown in the fourth column of Table 3.1. High values of this ratio indicate that the influx and outflux values are close to one another in magnitude, meaning that a small percentage error in the netflux estimate, may lead to a large percentage error in the netflux result.

Another source of error relevant to the analysis using Bradley data is that mean monthly flux values were used, meaning that transient eddy flux terms were not considered. When time averaging is done on the product of two time-varying quantities - like velocity and specific humidity in this case - eddy flux terms arise because of random variations in velocity and in specific humidity at time scales less than the averaging period used for the analysis. These eddy flux terms may have a significant influence on mass transport in certain situations. In their analysis of moisture flux into North and South America, Brubaker et al. decomposed the vertically integrated moisture flux into mean motion and transient eddy terms. They note that from a global perspective mean motion dominates  $Q_v$  while mean and transient eddy terms are of comparable magnitude in  $Q_w$ . From the results of their study, Brubaker et al. concluded that eddy flux terms contribute significantly to the north-south transport of water vapor, particularly along the Gulf of Mexico in the winter months. Thus, fluctuations on a few day time scale are important when considering the transport of water vapor, a conclusion also reached by Rasmusson, 1967.

3.3.3 Summary and Discussion

Two consistent methods for computing the divergence of atmospheric moisture using rawinsonde data have been described: one using a finite difference approximation on a spherical grid and one by summing fluxes across boundary lines. The results of these computations were compared with output from a general circulation model. In general, computations based strictly on observed data yielded poorer estimates of divergence, with the estimate of average annual divergence over Texas being 15 times greater than observed runoff. The divergence estimate from the general circulation model was about 5 times greater than observed runoff. Reasons for errors may include (1) the sparseness of observations, (2) errors associated with taking differences between large numbers, and (3) using monthly average flux values. With regard to the first reason for errors, improved observation networks and remote sensing may help to alleviate problems with data resolution in future studies. The United States National Meteorological Center is presently implementing a new mesoscale general circulation model over North America called the Eta model, using 40 km computational cells which will provide about 25 times greater horizontal resolution than the grid used in this study. The second problem may be difficult to overcome considering the large amounts of moisture that flow through the atmosphere relative to the amounts of precipitation, evaporation, and runoff. Statewide average estimates from this study indicate that the average annual throughflux (1973 - 1994) of atmospheric moisture is 7788 mm while the annual precipitation is 120 mm and average annual runoff is 78.4 mm (See Section 5). Indicating that only 9% of the moisture passing over the State falls as precipitation and 11% of this precipitation becomes runoff. With regard to the third problem, data for making calculations on shorter than monthly time steps are available, but were not used due to time and logistical constraints in this study.

When calculations made in this study were compared with the output of a National Meteorological Center GCM, the GCM results seemed more reasonable, but not entirely satisfactory. The GCM considers transient eddy behavior that is not captured by mean monthly observations because a much smaller time step is used. Simulation models also offer the advantage that equations of motion can be used to fill in areas with sparse observations. As products from higher resolution GCM simulations become available, simple operations in GIS can be used to estimate net fluxes into arbitrarily defined regions as done in this study.

Some additional information would have been useful to help assess the relative importance of different sources of error in this study. The use of 12 hourly data could have shed more light on problems associated with using monthly average values. It also would have been interesting to know the locations where rawinsonde observations were actually made. In addition, more water content computations could have been made to yield better evaporation estimates.

4.1 Methodology  
4.1.1 Model Description

The soil-water balance model uses a simple accounting scheme to predict soil-water storage, evaporation, and water surplus. Surplus precipitation which does not evaporate or retain in soil storage and includes both surface and sub-surface runoff. The conservation of mass equation for soil-water can be written as follows:

$$\frac{\partial \theta}{\partial t} = P - E - S \quad (4.1)$$

where  $\theta$  is soil moisture,  $P$  is precipitation,  $E$  is evaporation,  $v$  is soil velocity, and  $t$  is time. Horizontal motion of water on the land surface or in the soil is not considered by this model. Snow melt was also not considered in these computations, but this probably does not introduce significant error for a study in Texas. Willmott et al., 1985, describe a simple scheme that could be included to account for snow melt.

At first glance, it would seem that the most natural spatial unit to use in a soil-water balance model would be a soil map unit, but these map units are very irregular shapes and a wide range of sizes. Because climate data also play an important role in the soil-water balance, the cells generated when climate data are interpolated onto regular grids are a justifiable choice for use as the modeling units in the soil-water balance. Climate data interpolated onto 0.5 grid boxes are used in this study.

A major source of uncertainty in evaluating Equation 4.1 is estimating the evaporation. Estimation of evaporation is based upon knowledge of potential evapotranspiration, water-holding capacity of the soil, and a moisture extraction function. These concepts and a method for evaluating Equation 4.1 are described below. Special consideration of the potential evapotranspiration concept is provided in the Section 4.2.

4.1.2 Description of Input data  
4.1.2.1 Climate data

Global data sets of mean monthly temperature and precipitation interpolated to a 0.5 grid were obtained by anonymous ftp to the University of Delaware (climate.geog.udel.edu). These data are from the "Global Air Temperature and Precipitation Data Archive" compiled by D. Legates and J. Willmott. The precipitation estimates were on a regular 0.5 degree grid. The Texas data were obtained from the Texas State Climatologist's office. The Texas data were obtained from the Texas State Climatologist's office. The Texas data were obtained from the Texas State Climatologist's office.

Global estimates of "plant-extractable water capacity" have recently become available on a 0.5 grid (Dunne and Willmott, 1996). As used in this report, the term "plant-extractable water capacity" is equivalent to water-holding capacity. One reason given for developing this global database was to eliminate the need for acquiring spatially variable plant-extractable water capacity to soil-water balance computations made over large areas. Information about soil, clay, organic content, plant rooting depth, and horizon thickness was used to estimate the plant-extractable water capacity. Figure 4-1 shows the distribution of this parameter throughout Texas. The global average for this parameter is 85 mm while the average in Texas is 143 mm.

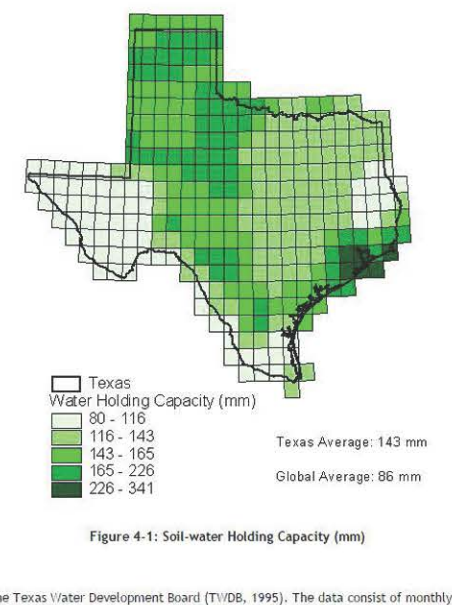


Figure 4-1: Soil-water Holding Capacity (mm)

4.1.2.2 Open Water Evaporation Estimates

Estimates of open water evaporation based upon evaporation measurements were provided by Alfredo Rodriguez at the Texas Water Development Board (TWDB, 1995). The data consist of monthly average gross reservoir evaporation estimates for one degree quadrangles in and around Texas. Monthly data for 1940 to 1990 are available in 75 quadrangles throughout Texas and monthly data for 1971-1990 in an additional 28 quadrangles at the border of Texas. Mean monthly evaporation values were computed from these data and used for estimates of potential evaporation in the soil-water balance calculations. Figure 4-2 shows the one degree quadrangle index map, shaded to indicate where data are available. Figure 4-3 shows mean annual reservoir evaporation. As an alternative, a global radiation data set described in the next section has recently become available that facilitates making potential evaporation estimates using the Priestley-Taylor equation. This method was also considered for use in the soil-water balance computations. An insightful comparison of these two methods for estimating potential evapotranspiration is described in Section 4.2.

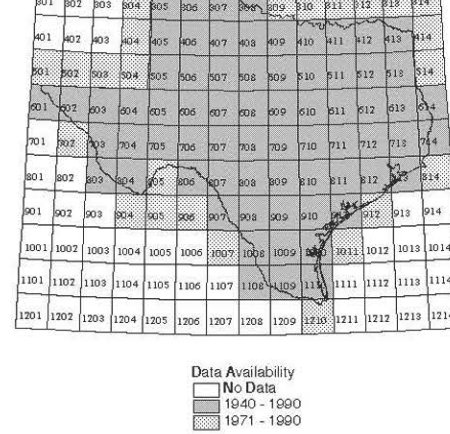


Figure 4-2: One Degree Quadrangle Index Map

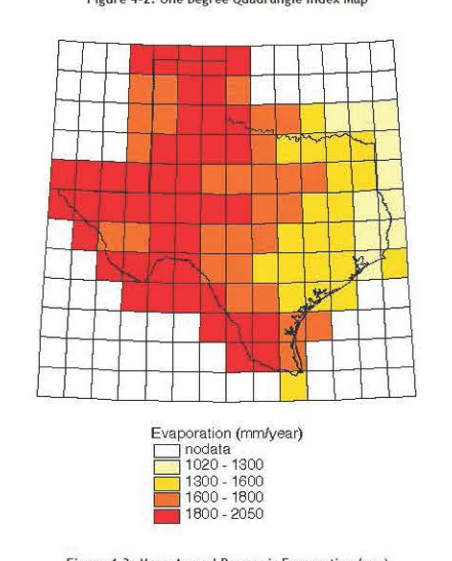


Figure 4-3: Mean Annual Reservoir Evaporation (mm)

4.1.2.3 Radiation data

A global radiation data set recently made available makes using the Priestley-Taylor method a feasible option for estimating potential evapotranspiration in large scale studies. These data are described by Darnell et al., 1995, and were obtained by anonymous ftp to cloud.larc.nasa.gov. The data set includes longwave and shortwave radiation flux estimates for a 96 month period extending from July 1983 to June 1991. The data are given on the ISCCP equal-area grid which has a spatial resolution of 2.5 at the equator. Darnell et al., 1995, describe advances in input data and flux estimation algorithms that improve the ability to assess the radiation budget on a global scale. Input data improvements have come from the International Satellite Cloud Climatology Project (ISCCP) and the Earth Radiation Budget Experiment (ERBE), using this satellite data, the radiation budget components that cannot be measured directly are estimated independently using physical approaches that have been validated against surface observations. According to Darnell et al., 1995, longwave flux estimates fall within +/- 25 W/m<sup>2</sup> of surface measurements while visible flux estimates are within +/- 20 W/m<sup>2</sup> of surface measurements. For comparison, the energy required to evaporate 1 mm/day of water is about 30 W/m<sup>2</sup>. In this study, net radiation (equivalent to net shortwave + net longwave) is used.

4.1.3 Water-holding capacity of the soil

In order to calculate the soil-water budget, an estimate of the soil's ability to store water is required. Several terms are used by soil scientists to define the water storage capacity of soils under different conditions. The field capacity or drained upper limit is defined as the water content of a soil that has reached equilibrium with gravity after several days of drainage. The field capacity is a function of soil texture and organic content. The permanent wilting point or lower limit of available water is defined as the water content at which plants can no longer extract a health sustaining quantity of water from the soil and begin to wilt. Typical suction values associated with the field capacity and wilting point are -10 kPa (0.1 bar) and -1500 kPa (-15 bar) respectively. Like water content, field capacity and permanent wilting point are defined on a volume of water per volume of soil basis. The water available for evapotranspiration after drainage (i.e. the available water-holding capacity) is defined as the field capacity minus the permanent wilting point. Table 4-1 gives some typical values for available water-holding capacity.

Table 4-1: Typical Values for Field-water Parameters by Texture\*

Texture Class	Field Capacity	Wilting Point	Available Capacity
Sand	0.12	0.04	0.08
Sandy Sand	0.14	0.08	0.06
Sandy Loam	0.23	0.10	0.13
Loam	0.26	0.12	0.14
Silt Loam	0.30	0.15	0.15
Silt	0.32	0.15	0.17
Silt Clay Loam	0.34	0.19	0.15
Silt Clay	0.36	0.21	0.15
Clay	0.36	0.21	0.15

\*Values obtained from ASCE, 1990, Table 2.6, p. 21.

For budgeting calculations, it is useful to know the total available water-holding capacity in a soil profile. This value is typically expressed in mm and can be obtained by integrating the available water-holding capacity over the effective depth of the soil layer. A one meter soil layer with a uniform available water-holding capacity of 15 has a total available water-holding capacity of 150 mm. For the remainder of this paper, the term water-holding capacity means total available water-holding capacity in units of mm. The water-holding capacity is denoted with  $w^*$  and the current level of moisture storage in the soil is denoted by  $w$ . A large water-holding capacity implies a large annual evapotranspiration and small annual runoff relative to a small water-holding capacity under the same climatic conditions.

4.1.4 Estimating Actual Evapotranspiration

To estimate the actual evapotranspiration in the soil-water budget method many investigators have used a soil-moisture extraction function or coefficient of evapotranspiration  $f$  which relates the actual rate of evapotranspiration to the potential rate of evapotranspiration based on some function of the current soil moisture content and the water-holding capacity.

$$E = f PE \quad (4.2)$$

Dick, 1983, Table 1 (reprinted in Shuttleworth, 1993, Table 4-4.4) provides a summary of some moisture extraction functions used by different investigators. Hitz and Walker, 1993, Figure 5, also illustrates several moisture extraction functions. Many researchers agree that soils show the general pattern of behavior that moisture is extracted from the soil at the potential rate until some critical moisture content is reached when evapotranspiration is no longer controlled by meteorological conditions. Below this critical point, there is a decline in soil moisture extraction until the wilting point is reached. This type of behavior is illustrated by Shuttleworth, 1993, Figure 4-4.3, p. 4-46 and Dingman, 1994, Figure 7-21. Shuttleworth, 1993, notes that the critical moisture content divided by the water-holding capacity is typically between 0.5 and 0.8. The type of moisture extraction function just described is commonly applied to situations when daily climate data are used. A simpler function in which the ratio of evapotranspiration to potential evapotranspiration is proportional to the current moisture level,  $f = w/w^*$ , has been applied when budgeting with monthly climate values and this function is used here.

There are drawbacks to using simple soil moisture extraction functions. Indices based on a function of soil moisture alone, do not account for the effects of vegetation. Minz and Walker, 1993, cite field studies that show  $f$  may vary with potential evapotranspiration for a given soil wetness and  $f$  may also vary with leaf-area index. In addition, the spatial variation of water-holding capacity is difficult to determine. A new and possibly better approach to determine the relationship between plant transpiration and potential evapotranspiration is to correlate  $f$  with satellite-derived indices of vegetation activity so that  $f$  may reflect plant growth stage and the spatial vegetation patterns. Gutman and Kulkovetz (1994) investigate this possibility. Using their approach still requires an estimate of potential evapotranspiration to get actual evapotranspiration.

4.1.5 Budgeting soil moisture to yield surplus

Soil-water budget calculations are commonly made using monthly or daily rainfall totals because of the way data are recorded. Computing the water balance on a monthly basis involves the unrealistic assumption that rain falls at constant low intensity throughout the month, and consequently surplus estimates made using monthly values are typically lower than those made using daily values. In dry locations, the mean potential evaporation for a given month may be higher than the commonly used value of zero surplus, even though there is some observed runoff. For this reason, the use of daily values is preferred over monthly values when feasible, yet daily budgeting still does not adequately describe storm runoff that occurs when the precipitation rate exceeds the infiltration capacity of the soil. One drawback to using daily data is that it is difficult to interpolate daily rainfall over space. For the state-wide study undertaken here, the use of daily data was deemed too cumbersome.

Equation 4.3 describes how soil moisture storage is computed.

$$w_1 = w_0 + P - f_1 PE \quad \text{if } w_1 < w^*$$

$$S_1 = w_1 - w^* \quad \text{and set } w_1 = w^* \quad \text{if } w_1 > w^* \quad (4.3)$$

In Equation 4.3,  $w_0$  is the current soil moisture,  $w_1$  is the soil moisture in the previous time step,  $P$  is precipitation,  $f_1$  is potential evapotranspiration,  $S_1$  is the surplus in a given day. If the soil moisture  $w_1$  is set equal to  $w^*$ , then the surplus for that day is  $w_1 - w^*$  and  $w_1$  is set equal to  $w^*$ . The soil-moisture extraction function  $f = w/w^*$  was used for this study.

4.1.6 Balancing Soil Moisture

If the initial soil moisture is unknown, which is typically the case, a balancing routine is used to force the net change in soil moisture from the beginning to the end of a specified balancing period (N time steps) to zero. To do this, the initial soil moisture is set to the water-holding capacity and budget calculations are made up to the time period (N-1). The initial soil moisture at time 1 ( $w_0$ ) is then set equal to the soil moisture at time N+1 ( $w_{N+1}$ ) and the budget is re-computed until the difference ( $w_0 - w_{N+1}$ ) is less than a specified tolerance.

4.2 Potential Evapotranspiration

4.2.1 Potential of the soil-water budget that involves significant uncertainty and ambiguity is estimating potential evapotranspiration. Just the concept of potential evapotranspiration is ambiguous by itself, as discussed in the next section. Two potential evapotranspiration estimates were considered for this study, gross evaporation and potential evaporation. Both estimates were made using the Priestley-Taylor equation. As discussed later, the gross reservoir evaporation estimates are considered to be better than the Priestley-Taylor estimates for use in the soil-water budget calculations.

4.2.2 Potential evaporation vs. potential evapotranspiration

Thornthwaite, 1948, first used the concept of potential evapotranspiration as a meaningful measure of moisture demand to replace two common surrogates for moisture demand, temperature and pan evaporation. Potential evapotranspiration refers to the maximum rate of evapotranspiration from a large area completely and uniformly covered with growing vegetation and with an unlimited moisture supply. There is a distinction between the term potential evapotranspiration and potential evaporation from a free water surface because factors such as stomatal impedance and plant growth stage influence evapotranspiration but do not influence potential evaporation from the free water surface.

Brutsaert, 1982, notes on pp. 214 and 221 the remarkable similarity in the literature among observations of water losses from short vegetated surfaces and free water surfaces. He poses a possible explanation that the stomatal impedance to water vapor diffusion in plants may be counterbalanced by larger roughness values. Significant differences have been observed between potential evapotranspiration from tall vegetation and potential evaporation from free water surfaces. The commonly used value of 1.26 in the Priestley-Taylor equation was derived using observations over both open water and saturated land surfaces. For the most part, the term potential evapotranspiration will be used in this paper and, as usual, includes water loss directly from the soil and/or through plant transpiration.

An additional ambiguity in using the potential evapotranspiration concept is that potential evapotranspiration is often computed based on meteorological data obtained under non-potential conditions (Brutsaert, p. 214). In this study, temperature and net radiation measurements used for calculating potential evapotranspiration in dry areas and for dry periods will be different than those that would have been observed under potential conditions. The fact that the Priestley-Taylor method exhibits weak performance at arid sites is related to this ambiguity because the assumptions under which the expressions were derived break down. This is particularly relevant to West Texas and is the main reason why evaporation estimates derived from pan coefficients are considered more applicable for the type of conditions being modeled in this study. A comparison of the two methods is described in Section 4.2.3.

Although not used directly in this study, a brief review of the widely used Penman equation serves as a good starting point for discussing the estimation of potential evapotranspiration.

4.2.3 Penman combination method

Two requirements for Bowen ratio as an energy input and a mechanism for the transport of water vapor from the saturated surface, in light of this, two traditional approaches to modeling evaporation are an energy budget approach and an aerodynamic approach. With the energy budget approach, the net radiation available at the surface (shortwave radiation absorbed less longwave radiation emitted) must be partitioned between latent heat flux and sensible heat flux, assuming that ground heat flux is negligible. This partitioning is typically achieved using the Bowen ratio which is the ratio of sensible heat flux to latent heat flux. Approximating the Bowen ratio typically requires measurements of temperature and humidity at two heights. The aerodynamic approach involves a vapor transport coefficient times the vapor pressure gradient between the saturated surface and an arbitrary measurement height. Determination of the vapor transport coefficient requires measurements of wind speed, humidity, and temperature. Brutsaert, Chow et al., and Dingman, present equations for calculating the Bowen ratio and vapor transport coefficients. Without simplifying assumptions, energy budget and the aerodynamic methods require meteorological measurements at two levels.

In 1948, Penman combined the energy budget and aerodynamic approaches. Penman's derivation eliminates the need for measuring water surface temperature; only the air temperature is required. The resulting equation is as follows:

$$E = \frac{\Delta}{\Delta + \gamma} B_e + \frac{\gamma}{\Delta + \gamma} B_w \quad (4.4)$$

where  $\Delta = \frac{d e}{d T}$ ,  $B_e = E_0(1 - \alpha_s)$ ,  $E_0$  is net radiation [ $W m^{-2}$ ],  $\alpha_s$  is latent heat of vaporization [ $J kg^{-1}$ ],  $\rho_w$  is density of water [ $kg m^{-3}$ ],  $K_{10}$  is a mass transfer coefficient,  $e_s$  is saturated vapor pressure at air temperature, and  $e$  is the actual vapor pressure.

The Penman equation is a weighted average of the rates of evaporation due to net radiation ( $E_0$ ) and turbulent mass transfer ( $E_w$ ). Provided that model assumptions are met and adequate input data are available, various forms of the Penman equation yield the most accurate estimates of evaporation from saturated surfaces. Shuttleworth, 1993, states that the Priestley-Taylor method is the "preferred radiation-based method for estimating reference crop evapotranspiration." Shuttleworth, 1993, notes that errors using the Priestley-Taylor method are on the order of 1% to 0.75 mm/day, whichever is greater, and that estimates should only be made for periods of ten days or longer.

4.2.3 Simpler Methods

Two simpler methods that are much easier to apply than forms of the Penman equation were considered in this study, a pan coefficient approach and the Priestley-Taylor method.

4.2.3.1 Pan coefficients

Evaporation pans are commonly used to estimate open water evaporation from nearby lakes and reservoirs. The rate of evaporation is estimated by measuring the change in water level with time. Lake evaporation is estimated by multiplying the pan evaporation by a pan coefficient. Typical values of the pan coefficient range from 0.67 to 0.78 in Texas, so the measured evaporation from the pan is higher than that from the lake surface. Pan coefficients vary with location and season. The development of gross reservoir evaporation estimates used in this study is described by TWDB, 1995. As discussed in Section 4.2.1, open water evaporation and potential evapotranspiration are often of similar magnitude, justifying the use of open water evaporation estimates in soil-water budget calculations.

4.2.3.2 Priestley-Taylor method

In 1972, C.B. Priestley and R.J. Taylor showed that, under certain conditions, knowledge of net radiation and ground dryness may be sufficient to determine vapor and sensible heat fluxes at the Earth's surface. When large land areas (on the order of hundreds of kilometers) become saturated, Priestley and Taylor derived accurate estimates of potential evapotranspiration. The Priestley-Taylor method is an incomplete hydrology model because it is very difficult to calibrate against observed values. Coupling a soil-water balance model with measured runoff is the only realistic way to derive accurate runoff estimates. A simplified method of the soil-water balance model was achieved in a recent study to develop a GIS-based water planning tool for the Niger River Basin in West Africa (Moukoko et al., 1994; <http://www.cerada.ahw.fr/gis/moukoko/GSDbnyr/africa/Africa.htm>). This model was calibrated for monthly flows but not validated. A more detailed approach to this type of study could be taken by implementing a continuous stream flow simulation model with daily time stepping (or less); however, implementing this type of model on a region the size of Texas is a formidable task.

4.2.3.3 Comparison of Pan and Priestley-Taylor methods

In 1972, C.B. Priestley and R.J. Taylor showed that, under certain conditions, knowledge of net radiation and ground dryness may be sufficient to determine vapor and sensible heat fluxes at the Earth's surface. When large land areas (on the order of hundreds of kilometers) become saturated, Priestley and Taylor derived accurate estimates of potential evapotranspiration. The Priestley-Taylor method is an incomplete hydrology model because it is very difficult to calibrate against observed values. Coupling a soil-water balance model with measured runoff is the only realistic way to derive accurate runoff estimates. A simplified method of the soil-water balance model was achieved in a recent study to develop a GIS-based water planning tool for the Niger River Basin in West Africa (Moukoko et al., 1994; <http://www.cerada.ahw.fr/gis/moukoko/GSDbnyr/africa/Africa.htm>). This model was calibrated for monthly flows but not validated. A more detailed approach to this type of study could be taken by implementing a continuous stream flow simulation model with daily time stepping (or less); however, implementing this type of model on a region the size of Texas is a formidable task.

Because the net radiation at the earth's surface is directly related to the wetness of the area, it may be a better surrogate for actual evapotranspiration than potential evapotranspiration. In Section 5.3.2 a map of Bowen ratios for Texas is computed. As discussed in this section, use of net radiation and temperature data, along with a map of Bowen ratios may be an alternative approach to estimating evaporation that eliminates the use of the difficult potential evapotranspiration concept.

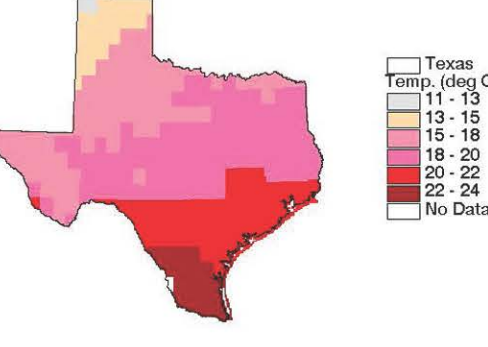


Figure 4-4: Mean Annual Temperature in Texas, from Legates and Willmott (1996)



Figure 4-5: Mean Annual Net Radiation Estimates from the ERBE Program

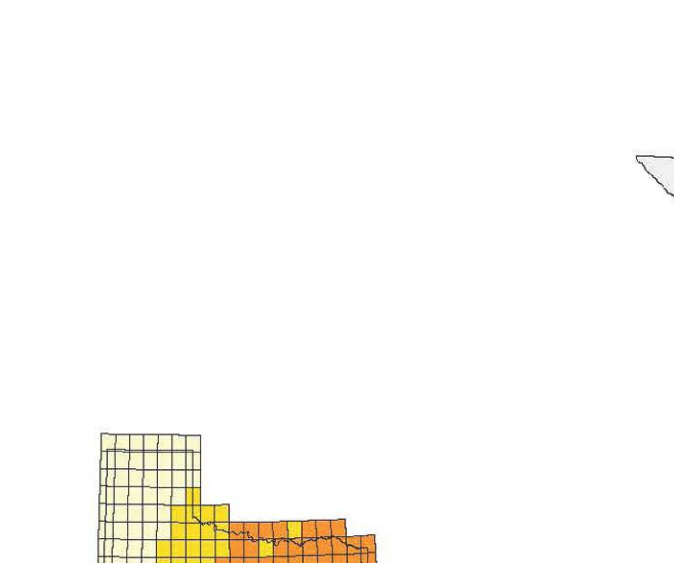


Figure 4-6: Priestley-Taylor Potential Evaporation (mm/year)

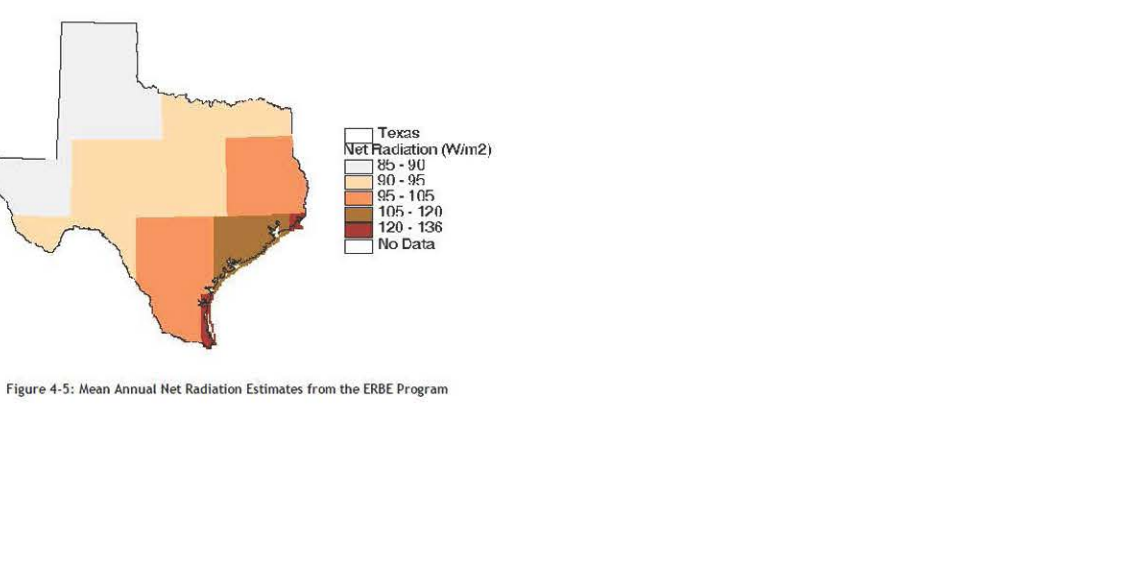


Figure 4-7: Soil-water balance Monthly Results for Two Cells

In terms of absolute magnitude, the statewide average reservoir evaporation is much higher (1690 mm year<sup>-1</sup>) than the Priestley-Taylor estimate (1120 mm year<sup>-1</sup>); however, the values in East Texas are more comparable because the lowest reservoir evaporation estimates and highest Priestley-Taylor estimates both occur here. Looking at the results of the next section, differences in the spatial and temporal distribution between the two potential evaporation estimates make a big difference in the resulting surplus.

4.3 Results

The results from the soil-water balance are monthly estimates of evaporation, surplus, and soil moisture in each 0.5 grid cell covering the State. Figure 4.7 shows the mean annual surplus estimated from two separate calculations, the first using the Priestley-Taylor potential evapotranspiration method and the second using the reservoir evaporation as potential evapotranspiration. Using the Priestley-Taylor potential evapotranspiration method yields an average of 85 mm year<sup>-1</sup> of surplus across the State while the use of the reservoir evaporation method yields 46.4 mm year<sup>-1</sup> and the observed runoff (78.4 mm year<sup>-1</sup> from Section 5) is somewhere between these two estimates. A major problem is that this soil-water balance model predicts zero runoff for much of the State even though it is known that some runoff occurs in these areas. The time distribution of precipitation, actual evaporation, soil moisture, and surplus for two cells are shown in Figure 4.8. In the cell on the left, the water-holding capacity (162.5 mm) is never reached, but for the cell on the right the water-holding capacity (91 mm) is exceeded during seven months out of the year and surplus is generated.

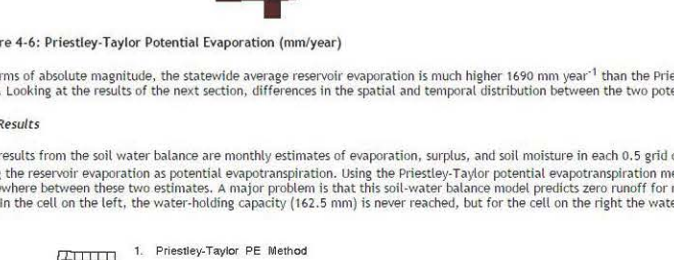


Figure 4-9: Annual Surplus from Soil-water Balance

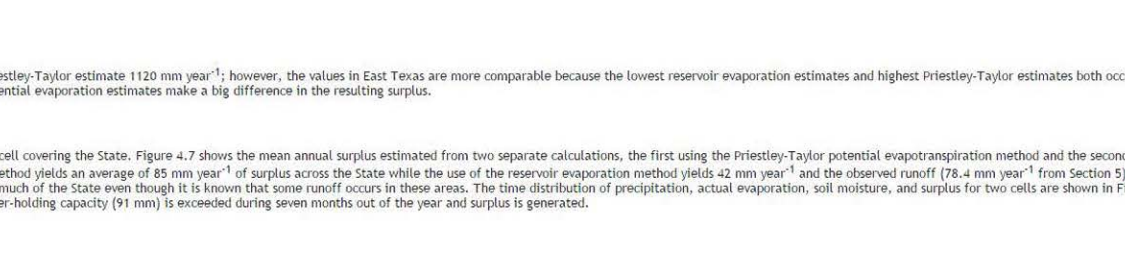


Figure 4-10: Mean Annual Saturated Fraction of Soil-water Holding Capacity

4.4 Summary

The rudimentary soil-water balance approach used in this study provides a qualitative sense of how precipitation is partitioned between runoff, evaporation, and soil moisture storage. The surplus and soil moisture values computed with this model are interpreted better as indices of relative wetness rather than absolute estimates because none are calibrated against measured values. Use of a monthly time step, a simplified representation of soil and plant biology, the ambiguity in applying the potential evapotranspiration concept to dry areas, and the errors in estimating potential evapotranspiration are major limitations of this model. The model time step cannot account for storm runoff, an important mechanism for runoff generation. The soil-water balance model is an incomplete hydrology model because it is very difficult to calibrate against observed values. Coupling a soil-water balance model with measured runoff is the only realistic way to derive accurate runoff estimates. A simplified method of the soil-water balance model was achieved in a recent study to develop a GIS-based water planning tool for the Niger River Basin in West Africa (Moukoko et al., 1994; <http://www.cerada.ahw.fr/gis/moukoko/GSDbnyr/africa/Africa.htm>). This model was calibrated for monthly flows but not validated. A more detailed approach to this type of study could be taken by implementing a continuous stream flow simulation model with daily time stepping (or less); however, implementing this type of model on a region the size of Texas is a formidable task.



## 6.0 CONCLUSIONS

Three water balance methods - an atmospheric water balance, a soil-water balance, and a surface water balance - have been used in an attempt to gain an improved understanding of the stocks of water in different components of the hydrologic cycle and the fluxes between these components. Long term average values indicate that the air flowing over Texas carries  $7800 \text{ mm year}^{-1}$  of moisture, of which  $720 \text{ mm year}^{-1}$  becomes precipitation, from which  $78 \text{ mm year}^{-1}$  becomes surface runoff, all of these quantities being spatially averaged over the State. The runoff estimate of  $78 \text{ mm year}^{-1}$  comes from the surface water balance which has the least uncertainty and highest spatial resolution of the three methods. Comparing mean annual runoff estimates from the other two methods to this figure is one way to assess the accuracy of these methods.

Given adequate data, the atmospheric water balance is a promising method for estimating regional evaporation, runoff, and changes in basin storage; however, data used in this study were not at a high enough resolution to make accurate calculations for Texas. Estimates of mean annual divergence over the State were made using both observed rawinsonde data and the output data from a general circulation model. Both methods show that there is significant uncertainty associated with atmospheric water balance calculations at the scale of Texas, yielding runoff estimates of  $1206 \text{ mm year}^{-1}$  and  $379 \text{ mm year}^{-1}$  which are about 15 times and 5 times greater than the observed runoff respectively. A review of literature indicates that the magnitude of the errors found in these calculations are not unheard of, although results for some regions have proven much more accurate, particularly when the water balance is assessed over larger areas. Assuming that

monthly changes in atmospheric storage are negligible, estimates of monthly evaporation were made for 1992 using the relation ( $E = \nabla \cdot \vec{Q} + P$ ). The 1992 evaporation estimates based on the observed data are not physically realistic while the estimates generated using the general circulation model output show reasonable monthly trends except in January, February, and March. Several sources of error were identified including the sparseness of observations, errors associated with taking the difference between two large numbers, and using monthly average flux values when a significant amount of mass transport can occur at smaller time scales. The contributions of the first and third sources of error mentioned here may be reduced as better data sets become available and if more detailed calculations are made.

The soil-water balance is a climatological approach which is instructive, but also contains substantial uncertainties. The main reasons for the uncertainties in the soil-water balance are a simplified representation of land surface hydrology, the use of monthly average rainfall data, and the fact that there is no calibration with observed data of either soil moisture or runoff. Because of these assumptions, the soil-water balance model predicts zero runoff over large areas of the State where surface runoff actually does occur. The soil-water balance does provide qualitative information about the space and time variability of soil moisture and evapotranspiration that are not revealed by the annual surface water balance, but a way to confirm these results has not been worked out.

Use of the soil-water balance requires an estimate of potential evapotranspiration. One approach taken to estimating potential evapotranspiration was to use the Priestley-Taylor method because a net radiation data set described by Darnell *et al.*, 1995, was available. The other approach was to use gross reservoir evaporation estimates (TWDB, 1995) derived using pan coefficients. As expected, the Priestley-Taylor method was not appropriate for arid areas in West Texas and it is seen that net radiation may be a better surrogate for actual evapotranspiration rather than potential evapotranspiration.

To facilitate the surface water balance, 166 USGS gaging stations were selected for analysis, and a 500 m digital elevation model was used to delineate the drainage areas for each gage. A 5 km grid of mean annual precipitation and mean annual runoff values compiled for each gage (both time averaged from 1961-1990) were used to derive a relationship between mean annual precipitation (mm) and the mean annual surface runoff (mm). This relationship is given in Equation 5.2 and applies in areas without unusually large groundwater recharge, springflow, urbanization, or reservoir impoundment. Applying this relationship to the precipitation grid, a grid of expected runoff was derived. While the precipitation in Texas ranges from about  $200 \text{ mm year}^{-1}$  in West Texas to  $1483 \text{ mm year}^{-1}$  in East Texas, the expected runoff varies from near 0 in West Texas to  $417 \text{ mm year}^{-1}$  in the wettest parts of East Texas.

In locations where information about observed flows was used, the differences between expected runoff and observed runoff could be determined, and Figure 5.14 is a map showing where deviations from expected runoff occur. On this map, areas where observed runoff is much higher than the expected runoff correspond to watersheds where inter-watershed transfers are received or urbanization has caused high runoff coefficients, while the areas where observed runoff is much lower than expected correspond to watersheds from which recharge is transferred to other watersheds or the impacts of agriculture are significant. Adding the grid of deviations from expected runoff to the grid of expected runoff yielded a grid of actual runoff for the State (Figure 5.15). Accumulated flow maps were also created, using these runoff maps and a 500 m digital elevation model to define the drainage network. Using various line colors and line thicknesses to represent accumulated flow, these maps reveal statewide spatial trends such as the increased density of stream networks in East Texas, while also capturing localized phenomena such as large springflows. The runoff grids developed in this study have several potential uses. The grid of observed runoff may be useful in estimating non point source pollution loads in a manner similar to that described by Saunders and Maidment, 1996. Use of the expected runoff grid or a similar grid may be helpful in assessing the amount of water available for human use. Accumulated flow maps may be useful in attributing digitized stream networks with flow data.

A grid of mean annual expected evaporation was estimated by subtracting the grid of expected runoff from the precipitation grid. The values of expected evaporation range from  $200 \text{ mm year}^{-1}$  in West Texas to  $1066 \text{ mm year}^{-1}$  in East Texas. Using the evaporation grid, the net radiation grid, and a temperature grid, a map of mean annual Bowen ratios for the State was created. These Bowen ratio values vary from 4.6 in West Texas (sensible heating of air dominates evaporation in a dry area) to 0.24 in East Texas (latent heat absorbed by evaporation dominates over sensible heating of air in a wet area).

As spatial data sets from remote sensing continue to improve along with tools like a GIS for manipulating spatial data, hydrologists can think in terms of water maps both in the atmosphere and on the land surface rather than thinking just in terms of point measurements. Working with a GIS allows for the computation of water balances on arbitrary control volumes and simplifies the use of complex spatial data. A large amount of data for the state of Texas has been compiled during this study, and this data will be useful to others in the future. A CD-ROM is available from the Center for Research in Water Resources (CRWR), University of Texas at Austin, that contains the data and programs used to make the computations described in this report. A description of the contents of this CD-ROM is provided in the Appendix to this report. Data used to plot the figures presented in this report are included on this CD-ROM and these data files are indexed in Part C of the Appendix.

## 7.0 ACKNOWLEDGEMENT

This research was sponsored by the Texas Water Resources Institute and the U.S. Geological Survey under Project 5903. The authors wish to acknowledge the advice and assistance of Allen Bradley of the Iowa Institute for Hydraulic Research, Alfredo Rodriguez of the Texas Water Development Board, Cort Willmott of the University of Delaware, and Sam Atkinson of the University of North Texas.

## 8.0 REFERENCES

1. Alley, W.M., "On The Treatment Of Evapotranspiration, Soil Moisture Accounting, and Aquifer Recharge in Monthly Water Balance Models," *Water Resources Research*, **20**,1137-1149,1984
2. Arnell, N.W., "Grid Mapping of River Discharge," *Journal of Hydrology*, **167**, 39-56, 1995.
3. Atkinson, S.F., J.R. Thomlinson, B.A. Hunter, J.M. Coffey, and K.L. Dickson, "The DRASTIC Groundwater Pollution Potential of Texas," prepared by The Center for Remote Sensing and Landuse Analyses Institute of Applied Sciences, University of North Texas, Denton, Texas, September, 1992.
4. Atkinson, S.F., J.R. Thomlinson, "An Examination of Ground Water Pollution Potential Through GIS Modeling," ASPRS/ACSM Annual Convention and Exposition : Technical Papers, Reno, Nevada, 1994.
5. ASCE, *Evapotranspiration and Irrigation Water Requirements*, Jensen, M.E., R.D. Burman, and R.G. Allen (editors), ASCE Manuals and Reports on Engineering Practice No. 70, 1990.
6. Brubaker, K.L., D. Entekhabi, and P.S. Eagleson, "Atmospheric Water Vapor Transport and Continental Hydrology over the Americas," *Journal of Hydrology*, **155**, 407-428, 1994.
7. Brutsaert, W., *Evaporation into the Atmosphere: Theory, History, and Applications*, D. Reidel Publishing Company, Dordrecht, Holland, 1982.
8. Chow, V.T., D.R. Maidment, and L.W. Mays, *Applied Hydrology*, McGraw-Hill, Inc., New York, NY, 1988.
9. Church, M. R., G.D. Bishop, and D.L. Cassell, "Maps of Regional Evapotranspiration and Runoff/Precipitation Ratios in the Northeast United States," *Journal of Hydrology*, **168**, 283-298, 1995.
10. Daly, C., R. Neilson, and D. Phillips, "A Statistical-Topographic Model for Mapping Climatological Precipitation over Mountainous Terrain," *Journal of Applied Meteorology* , **33**, 2, February 1994.
11. Darnell, W.L., W.F. Staylor, S.K. Gupta, N.A. Ritchey, and A.C. Wilber, "Seasonal Variation of Surface Radiation Budget Derived from ISCCP-C1 Data," *J. Geophysical. Res.*, **97**, 15741-15760, 1992.
12. Darnell, W.L., W.F. Staylor, S.K. Gupta, N.A. Ritchey, and A.C. Wilber, "A Global Long-term Data Set of Shortwave and Longwave Surface Radiation Budget," GEVEX News, **5**, No.3, August 1995.
13. Dingman, S.L., *Physical Hydrology*, Prentice Hall, Inc., Englewood Cliffs, NJ, 1994.
14. Dugas, W.A., and C.G. Ainsworth, *Agroclimatic Atlas of Texas*, Part 6: Potential Evapotranspiration, Report MP 1543, Texas Agricultural Experiment Station, College Station, December, 1983.
15. Dyck, S., "Overview on the Present Status of the Concepts of Water Balance Models," *New Approaches in Water Balance Computations* (Proceedings of the Hamburg Workshop), IAHS Publ. No. 148, 1983.
16. Dunne, K.A., and C.J. Willmott, "Global Distribution of Plant-extractable Water Capacity of Soil," *International Journal of Climatology*, **16**, 841-859, 1996.
17. "Global Energy and Water Cycle Experiment (GEWEX) News," World Climate Research Programme, August, 1995, V. 5, No. 3.
18. Gutman, G., and L. Rukhovetz, "Towards Satellite-Derived Global Estimation of Monthly Evapotranspiration Over Land Surfaces," *Adv. Space Res.*, **18**, No. 7, 67-71, 1996.
19. Hydrodata CD-ROM, "NCDC Summary of the Day - West 2," Hydrosphere, Boulder, CO, 1994.
20. Hydrodata CD-ROM, "USGS Daily Values - West 2," Hydrosphere, Boulder, CO, 1994.
21. Kreyszig, E., *Advanced Engineering Mathematics*, 7<sup>th</sup> Edition, John Wiley and Sons, Inc., 1993.
22. Legates, D.R., and Willmott, C.J., "Mean Seasonal and Spatial Variability in Gauge-Corrected, Global Precipitation," *International Journal of Climatology*, **10**, 111-127, 1990.
23. Lullwitz, T. and A. Helbig, "Grid Related Estimates of Streamflow within the Weser River Basin, Germany," Modeling and Management of Sustainable Basin-scale Water Resource Systems, Symposium Proceedings, Boulder, Colorado, IAHS Publ. No. 231, 1995.
24. Maidment, D.R., "GIS and Hydrologic Modeling - an Assessment of Progress," <http://www.ce.utexas.edu/prof/maidment/GISHydro/meetings/santafe/santafe.html>.
25. Maidment, D.R., F. Olivera, Z. Ye, S. Reed, and D.C. McKinney, "Water Balance of the Niger Basin," accepted for publication in the Proceedings of the ASCE North American Water and Environment Congress '96, Anaheim, CA, 1996.
26. Manabe, Syukuro, "Climate and the Ocean Circulation: I. The Atmospheric Circulation and the Hydrology of the Earth's Surface," *Monthly Weather Review*, **97**, No. 11, Nov. 1969.
27. Mather, J.R., *The Climatic Water Budget*, Lexington Books, 1972.
28. Mintz, Y., and Serafini, Y.V., "A Global Monthly Climatology of Soil Moisture and Water Balance," *Climate Dynamics*, **8**, 13-27, 1992.
29. Mintz, Y., and G.K. Walker, "Global Fields of Soil Moisture and Land Surface Evapotranspiration Derived from Observed Precipitation and Surface Air Temperature," *J. Applied. Meteor.*, **32**, 1305-1334, 1993.
30. Oki, T., K. Musiaka, H. Matsuyama, K. Masuda, "Global Atmospheric Water Balance and Runoff from Large River Basins," *Scale Issues in Hydrological Modeling*, Chapter 24, 411-434, 1994.
31. Patoux, Jerome, "Atmospheric Water Balance of Texas," Departmental Report, Environmental and Water Resources Engineering, University of Texas at Austin, December 1994.
32. Penman, H.L., "Natural Evaporation from Open Water, Bare Soil and Grass," *Proc. R. Soc. London, Ser. A*, **193**, 120-145, 1948.
33. Priestley, C.H.B., and R.J. Taylor, "On the Assessment of Surface Heat Flux and Evaporation Using Large-Scale Parameters," *Monthly Weather Review*, **100**, No. 2, 81-92, February 1972.
34. Rasmusson, E.M., "Atmospheric Water Vapor Transport and the Water Balance of North America: Part 1. Characteristics of the Water Vapor Flux Field," *Monthly Weather Review*, **95**, 7, pp. 403-426, July 1967.
35. Saunders, W.K., and D.R. Maidment, "A GIS Assessment of Nonpoint Source Pollution in the San Antonio-Nueces Coastal Basin," Online Report 96-1, Center for Research in Water Resources, University of Texas at Austin.
36. Shuttleworth, J.W., "Evaporation," Handbook of Hydrology, D.R. Maidment Editor, McGraw-Hill, Inc., 1993.
37. Shiklomanov, A., and A.A. Sokolov, "Methodological Basis of World Water Balance Investigation and Computation," *New Approaches in Water Balance Computations* (Proceedings of the Hamburg Workshop), IAHS Publ. No. 148, 1983.
38. Smith, P.H., "Hydrologic Data Development System," Master's Thesis, University of Texas at Austin, August, 1995.
39. Snyder, J.P., "Map Projections a Working Manual," Professional Paper 1395, U.S. Geological Survey, Washington, D.C., 1987.
40. Thornthwaite, C.W., "An Approach Toward a Rational Classification of Climate," *Geographical Review*, **38**, 55-94, 1948.
41. TBWE Bulletin 6001, "Surface Runoff from Texas Watersheds and Basins," by Lockwood, Andrews, and Newman Consulting Engineers for the Texas Board of Water Engineers, February, 1960.
42. TDWR Report LP-192, "Climatic Atlas of Texas," Larkin, T.J. and G.W. Bomar, December 1983.
43. TVVDB Report 64, "Monthly Reservoir Evaporation Rates for Texas 1940 through 1965," Kane, J.W., October, 1967.
44. TVVDB Report 189, "Major and Historical Springs of Texas," Brune, G., March, 1975.
45. TVVDB Report 238, "Groundwater Availability in Texas : Estimates and Projections through 2030," Muller, D.A., and Price, R.D. 1979.
46. TVVDB, "Water for Texas Today and Tomorrow," 1990.
47. TVVDB, "Monthly Reservoir Evaporation Rates for Texas Using GIS THEVAP Model," August, Rodriguez, A., 1995.
48. Ward, G.H., "A Water Budget for the State of Texas with Climatological Forcing," *Texas Journal of Science*, **45**, No. 3, 249-264, 1993.
49. Whitlock *et al.*, "First Global WCRP Shortwave Surface Radiation Budget Data Set," *Bull. Amer. Meteor. Soc.*, **76**, 6, 905-922, 1995.
50. Wiln, H.G., C.W. Thornthwaite, E.A. Colman, N.W. Cummings, A.R. Croft, H.T. Gisborne, S.T. Harding, A.H. Hendrickson, M.D. Hoover, I.E. Houk, J. Kittredge, C.H. Lee, C.G. Rossby, T. Saville, and C.A. Taylor, "Report of the Committee on Transpiration and Evaporation, 1943-44," *Transactions, American Geophysical Union*, **25**, 683, 1944.
51. Willmott, C.J., C.M. Rowe, and Y. Mintz, "Climatology of the Terrestrial Seasonal Water Cycle," *Journal of Climatology*, **5**, 589-606, 1985.
52. Willmott, C.J., "WATBUG: A FORTRAN IV Algorithm for Calculating the Climatic Water Budget," *Publications in Climatology*, **30**, 2, 1977.

# APPENDIX

**General Information**  
The data and programs used in this study are available on a CD-ROM from the Center for Research in Water Resources (CRWR), University of Texas at Austin. This appendix contains general information about the CD-ROM contents, an overview of the directory structure, a listing of figures and the data files used to create them, and a description of all data files and programs.

As this research project has progressed, programs developed at different times vary significantly in the quality of comments and flexibility of application. Many of the programs will require some changes if they are to operate on data sets other than those for which they were originally written. Programmers may find extra programs or sections of programs useful, but only a few of the programs are written for the casual user to simply copy and run.

The main directory on the CD-ROM is TEXAS. This directory contains a "header" file that provides a brief description of all data files and programs, including sub-directories. Most sub-directories also contain a file called "subdir" which explains procedures used to develop data sets and make calculations. There are also files called "subdir1", "subdir2", etc., which are more succinct versions of "subdir".

Listing of data files and programs with the parameters for the Texas State Mapping System. When possible, data sources were transformed to HDR3; however, errors associated with blocks of data are negligible when considering the scale of the data used in this study. Here are the project parameters used in this study.

**projection aliases**  
units meters  
datum north  
parameters  
27 25 00  
14 50 00  
100 00 00  
100000.0  
100000.0  
end

A few coverages used in the atmospheric water balance are an all-area projection with parameters typically used for national maps of the United States. This is sometimes referred to as the "national" all-area projection in file descriptions below. The projection description for these coverages is as follows:

**projection aliases**  
units meters  
datum north  
parameters  
27 25 00  
14 50 00  
100 00 00  
100000.0  
100000.0  
end

**B. Key Sub-directories**  
Here is a brief description of key subdirectories. The complete contents of these directories are listed in Appendix D.

**ATMORAL:** files used to make atmospheric water balance calculations.  
**AVTFILES:** Arcview scripts.  
**BASINS:** data and programs involved in the process of watershed and stream delineation; delineated watersheds (tomb3-2) with attributes used to derive expected runoff function (Section 5.3.1).  
**BEADNET:** contains a copy of this report in both Microsoft Word and HTML format.  
**BSMAPS:** programs and data files used in computing the soil-water balance (Chapter 4).  
**STRMS:** coverage and major figures in Texas were created based on information taken from T-108 Report 189 by Gunnar Brown. A set of attributes including name, maximum observed flow, and the year that this maximum flow was observed has been compiled for each spring.  
**HS2000:** cross-section data extracted from a hydrographer CD-ROM; points coverage of stream gage localities with relevant information such as mean monthly and mean annual flow; a number of Arcview scripts including scripts to manage data extracted from the hydrographer CD-ROM; to make unit conversions, and to assist in computing potential inflow and net measured flow in this study.

**C. Listing of data files and programs presented in this report**

The following table gives the data files that were used to create figures in this report. The symbol indicates the file's "parent" directory which varies with systems and is dependent on the identity of the CD-ROM drive. Figures that were not created using GIS data may not be listed. The name of the project file used to create the figure is also shown, but only if the pathnames in the project file must be changed in order to successfully open these projects on a system different than that on which they were developed. As used on the CD-ROM, all of these projects reference pathnames that begin with "Home\name\proj".

Figure #	Project File	Data Source File
1.1	~/atmoral/average.apr	~/atmoral/fradlay/fragpt, ~/atmoral/tomb2gp
1.2	~/atmoral/average.apr	~/atmoral/fradlay/fragpt, ~/atmoral/tomb2gp
1.3	~/atmoral/average.apr	~/atmoral/fradlay/fragpt, ~/atmoral/tomb2gp
1.4	~/atmoral/average.apr	~/atmoral/fradlay/fragpt, ~/atmoral/tomb2gp
1.5	~/atmoral/average.apr	~/atmoral/fradlay/fragpt, ~/atmoral/tomb2gp
1.6	~/atmoral/average.apr	~/atmoral/fradlay/fragpt, ~/atmoral/tomb2gp
1.7	~/atmoral/average.apr	~/atmoral/fradlay/fragpt, ~/atmoral/tomb2gp
1.8	~/atmoral/average.apr	~/atmoral/fradlay/fragpt, ~/atmoral/tomb2gp
1.9	~/atmoral/average.apr	~/atmoral/fradlay/fragpt, ~/atmoral/tomb2gp
1.10	~/atmoral/average.apr	~/atmoral/fradlay/fragpt, ~/atmoral/tomb2gp
1.11	~/atmoral/average.apr	~/atmoral/fradlay/fragpt, ~/atmoral/tomb2gp
1.12	~/atmoral/average.apr	~/atmoral/fradlay/fragpt, ~/atmoral/tomb2gp
1.13	~/atmoral/average.apr	~/atmoral/fradlay/fragpt, ~/atmoral/tomb2gp
1.14	~/atmoral/average.apr	~/atmoral/fradlay/fragpt, ~/atmoral/tomb2gp
1.15	~/atmoral/average.apr	~/atmoral/fradlay/fragpt, ~/atmoral/tomb2gp
1.16	~/atmoral/average.apr	~/atmoral/fradlay/fragpt, ~/atmoral/tomb2gp
1.17	~/atmoral/average.apr	~/atmoral/fradlay/fragpt, ~/atmoral/tomb2gp
1.18	~/atmoral/average.apr	~/atmoral/fradlay/fragpt, ~/atmoral/tomb2gp
1.19	~/atmoral/average.apr	~/atmoral/fradlay/fragpt, ~/atmoral/tomb2gp
1.20	~/atmoral/average.apr	~/atmoral/fradlay/fragpt, ~/atmoral/tomb2gp
1.21	~/atmoral/average.apr	~/atmoral/fradlay/fragpt, ~/atmoral/tomb2gp
1.22	~/atmoral/average.apr	~/atmoral/fradlay/fragpt, ~/atmoral/tomb2gp
1.23	~/atmoral/average.apr	~/atmoral/fradlay/fragpt, ~/atmoral/tomb2gp
1.24	~/atmoral/average.apr	~/atmoral/fradlay/fragpt, ~/atmoral/tomb2gp
1.25	~/atmoral/average.apr	~/atmoral/fradlay/fragpt, ~/atmoral/tomb2gp
1.26	~/atmoral/average.apr	~/atmoral/fradlay/fragpt, ~/atmoral/tomb2gp
1.27	~/atmoral/average.apr	~/atmoral/fradlay/fragpt, ~/atmoral/tomb2gp
1.28	~/atmoral/average.apr	~/atmoral/fradlay/fragpt, ~/atmoral/tomb2gp
1.29	~/atmoral/average.apr	~/atmoral/fradlay/fragpt, ~/atmoral/tomb2gp
1.30	~/atmoral/average.apr	~/atmoral/fradlay/fragpt, ~/atmoral/tomb2gp
1.31	~/atmoral/average.apr	~/atmoral/fradlay/fragpt, ~/atmoral/tomb2gp
1.32	~/atmoral/average.apr	~/atmoral/fradlay/fragpt, ~/atmoral/tomb2gp
1.33	~/atmoral/average.apr	~/atmoral/fradlay/fragpt, ~/atmoral/tomb2gp
1.34	~/atmoral/average.apr	~/atmoral/fradlay/fragpt, ~/atmoral/tomb2gp
1.35	~/atmoral/average.apr	~/atmoral/fradlay/fragpt, ~/atmoral/tomb2gp
1.36	~/atmoral/average.apr	~/atmoral/fradlay/fragpt, ~/atmoral/tomb2gp
1.37	~/atmoral/average.apr	~/atmoral/fradlay/fragpt, ~/atmoral/tomb2gp
1.38	~/atmoral/average.apr	~/atmoral/fradlay/fragpt, ~/atmoral/tomb2gp
1.39	~/atmoral/average.apr	~/atmoral/fradlay/fragpt, ~/atmoral/tomb2gp
1.40	~/atmoral/average.apr	~/atmoral/fradlay/fragpt, ~/atmoral/tomb2gp
1.41	~/atmoral/average.apr	~/atmoral/fradlay/fragpt, ~/atmoral/tomb2gp
1.42	~/atmoral/average.apr	~/atmoral/fradlay/fragpt, ~/atmoral/tomb2gp
1.43	~/atmoral/average.apr	~/atmoral/fradlay/fragpt, ~/atmoral/tomb2gp
1.44	~/atmoral/average.apr	~/atmoral/fradlay/fragpt, ~/atmoral/tomb2gp
1.45	~/atmoral/average.apr	~/atmoral/fradlay/fragpt, ~/atmoral/tomb2gp
1.46	~/atmoral/average.apr	~/atmoral/fradlay/fragpt, ~/atmoral/tomb2gp
1.47	~/atmoral/average.apr	~/atmoral/fradlay/fragpt, ~/atmoral/tomb2gp
1.48	~/atmoral/average.apr	~/atmoral/fradlay/fragpt, ~/atmoral/tomb2gp
1.49	~/atmoral/average.apr	~/atmoral/fradlay/fragpt, ~/atmoral/tomb2gp
1.50	~/atmoral/average.apr	~/atmoral/fradlay/fragpt, ~/atmoral/tomb2gp
1.51	~/atmoral/average.apr	~/atmoral/fradlay/fragpt, ~/atmoral/tomb2gp
1.52	~/atmoral/average.apr	~/atmoral/fradlay/fragpt, ~/atmoral/tomb2gp
1.53	~/atmoral/average.apr	~/atmoral/fradlay/fragpt, ~/atmoral/tomb2gp
1.54	~/atmoral/average.apr	~/atmoral/fradlay/fragpt, ~/atmoral/tomb2gp
1.55	~/atmoral/average.apr	~/atmoral/fradlay/fragpt, ~/atmoral/tomb2gp
1.56	~/atmoral/average.apr	~/atmoral/fradlay/fragpt, ~/atmoral/tomb2gp
1.57	~/atmoral/average.apr	~/atmoral/fradlay/fragpt, ~/atmoral/tomb2gp
1.58	~/atmoral/average.apr	~/atmoral/fradlay/fragpt, ~/atmoral/tomb2gp
1.59	~/atmoral/average.apr	~/atmoral/fradlay/fragpt, ~/atmoral/tomb2gp
1.60	~/atmoral/average.apr	~/atmoral/fradlay/fragpt, ~/atmoral/tomb2gp
1.61	~/atmoral/average.apr	~/atmoral/fradlay/fragpt, ~/atmoral/tomb2gp
1.62	~/atmoral/average.apr	~/atmoral/fradlay/fragpt, ~/atmoral/tomb2gp
1.63	~/atmoral/average.apr	~/atmoral/fradlay/fragpt, ~/atmoral/tomb2gp
1.64	~/atmoral/average.apr	~/atmoral/fradlay/fragpt, ~/atmoral/tomb2gp
1.65	~/atmoral/average.apr	~/atmoral/fradlay/fragpt, ~/atmoral/tomb2gp
1.66	~/atmoral/average.apr	~/atmoral/fradlay/fragpt, ~/atmoral/tomb2gp
1.67	~/atmoral/average.apr	~/atmoral/fradlay/fragpt, ~/atmoral/tomb2gp
1.68	~/atmoral/average.apr	~/atmoral/fradlay/fragpt, ~/atmoral/tomb2gp
1.69	~/atmoral/average.apr	~/atmoral/fradlay/fragpt, ~/atmoral/tomb2gp
1.70	~/atmoral/average.apr	~/atmoral/fradlay/fragpt, ~/atmoral/tomb2gp
1.71	~/atmoral/average.apr	~/atmoral/fradlay/fragpt, ~/atmoral/tomb2gp
1.72	~/atmoral/average.apr	~/atmoral/fradlay/fragpt, ~/atmoral/tomb2gp
1.73	~/atmoral/average.apr	~/atmoral/fradlay/fragpt, ~/atmoral/tomb2gp
1.74	~/atmoral/average.apr	~/atmoral/fradlay/fragpt, ~/atmoral/tomb2gp
1.75	~/atmoral/average.apr	~/atmoral/fradlay/fragpt, ~/atmoral/tomb2gp
1.76	~/atmoral/average.apr	~/atmoral/fradlay/fragpt, ~/atmoral/tomb2gp
1.77	~/atmoral/average.apr	~/atmoral/fradlay/fragpt, ~/atmoral/tomb2gp
1.78	~/atmoral/average.apr	~/atmoral/fradlay/fragpt, ~/atmoral/tomb2gp
1.79	~/atmoral/average.apr	~/atmoral/fradlay/fragpt, ~/atmoral/tomb2gp
1.80	~/atmoral/average.apr	~/atmoral/fradlay/fragpt, ~/atmoral/tomb2gp
1.81	~/atmoral/average.apr	~/atmoral/fradlay/fragpt, ~/atmoral/tomb2gp
1.82	~/atmoral/average.apr	~/atmoral/fradlay/fragpt, ~/atmoral/tomb2gp
1.83	~/atmoral/average.apr	~/atmoral/fradlay/fragpt, ~/atmoral/tomb2gp
1.84	~/atmoral/average.apr	~/atmoral/fradlay/fragpt, ~/atmoral/tomb2gp
1.85	~/atmoral/average.apr	~/atmoral/fradlay/fragpt, ~/atmoral/tomb2gp
1.86	~/atmoral/average.apr	~/atmoral/fradlay/fragpt, ~/atmoral/tomb2gp
1.87	~/atmoral/average.apr	~/atmoral/fradlay/fragpt, ~/atmoral/tomb2gp
1.88	~/atmoral/average.apr	~/atmoral/fradlay/fragpt, ~/atmoral/tomb2gp
1.89	~/atmoral/average.apr	~/atmoral/fradlay/fragpt, ~/atmoral/tomb2gp
1.90	~/atmoral/average.apr	~/atmoral/fradlay/fragpt, ~/atmoral/tomb2gp
1.91	~/atmoral/average.apr	~/atmoral/fradlay/fragpt, ~/atmoral/tomb2gp
1.92	~/atmoral/average.apr	~/atmoral/fradlay/fragpt, ~/atmoral/tomb2gp
1.93	~/atmoral/average.apr	~/atmoral/fradlay/fragpt, ~/atmoral/tomb2gp
1.94	~/atmoral/average.apr	~/atmoral/fradlay/fragpt, ~/atmoral/tomb2gp
1.95	~/atmoral/average.apr	~/atmoral/fradlay/fragpt, ~/atmoral/tomb2gp
1.96	~/atmoral/average.apr	~/atmoral/fradlay/fragpt, ~/atmoral/tomb2gp
1.97	~/atmoral/average.apr	~/atmoral/fradlay/fragpt, ~/atmoral/tomb2gp
1.98	~/atmoral/average.apr	~/atmoral/fradlay/fragpt, ~/atmoral/tomb2gp
1.99	~/atmoral/average.apr	~/atmoral/fradlay/fragpt, ~/atmoral/tomb2gp
2.00	~/atmoral/average.apr	~/atmoral/fradlay/fragpt, ~/atmoral/tomb2gp

**D. Description of files by directory**

**TEXAS (MAIN DIRECTORY)**  
**PROJECT FILES (.APR):**  
**NOTE:** Almost all project files assume that the pathnames for files start with "Home\name\proj". Most of these project files could be opened using data from the CD-ROM if the project paths are re-written to reflect the paths on which the CD-ROM is mounted.  
**figures.apr:** contains recharge figure for report and other figures used in presentations but not in report.  
**interp.apr:** contains layouts of accumulated expected and actual runoff in the San Antonio and Guadalupe basins.  
**plot.apr:** contains layout for Figure 1.1.  
**result.apr, result2.apr:** several versions of a project which load much of the spatial data associated with Texas. These projects also load several useful scripts. **Result2.apr** is the most recent version. Using this project, queries on watersheds were made to evaluate criteria for the expected runoff function. See Section 5.1.1.  
**run.apr:** project file used to map grids of results; displays the results of the runoff and evaporation grids that have been reorganized and converted to polygon coverages for display; used to create Figures 5.13, 5.14, 5.15, and 5.21 in final report.  
**runoff.apr:** this project file contains layouts used to create Figures 5.15, 5.16, and 5.17 in the final report.  
**tbl01.apr:** project used to create Table 5.1 in the final report.

**TEXT OR DBASE FILES:**  
**inf.txt:** list of watershed grid codes, mean rainfall, and mean runoff selected to create expected runoff function.  
**all.txt:** list of all 164 watershed grid codes, mean rainfall, and mean runoff values.  
**area36.txt:** list of grid used to check the consistency between areas reported by the USGS and areas delineated from the 500 m DEM.  
**area7.txt:** contains grid codes, DEM area, fraction error between DEM and USGS areas.  
**area7.txt:** contains grid codes, DEM area, fraction error between DEM and USGS areas.

**check3.txt:** created by check3.apr to compare flow at outlet points in actual runoff grid with observed flow at USGS gaging stations to make sure that runoff mapping method worked.  
**notes:** general description of the data on this file.  
**town.apr:** projection used to transform coordinates from geographic space to coordinates in the all-area projection with the parameters of the Texas State Mapping System.

**ATMORAL**  
**PROGRAMS:**  
**arow.apr:** draw Arcview graphics proportional in length to the moisture flux across a boundary segment; program called by plotflux.apr.  
**atmoral.apr:** computes the atmospheric, water balance for a region; required inputs are qdiff.txt and qdiff.txt which are created using ref1.f and header.apr.  
**~/atmoral/ref1.f:** reformats raw data files of moisture flux at the boundary points into a format that can be read into ArcView as Text files.  
**~/atmoral/ref1.f:** reformats raw data files of moisture flux at 2 degree grid points into a format that can be read into ArcView as Text files.  
**~/atmoral/theta.apr:** used to generate map of 2 degree polygon boundaries in projected space.  
**calcflow.apr:** computes the actual lengths of the x and y components of the Texas boundary segments given the latitude and longitude of segment endpoints (based on the Clarke 1866 ellipsoid).  
**convert.txt:** convert text series table of divergence values for cells into a time series of divergence values for the state; input table is ddivad.txt and output table is plotdivad.txt.  
**diverge.apr:** calculate divergence based on coordinates in point coverage polygons and data in file qdiff.txt and qdiff.txt; evaluates Equation 3.7; output table is ddivad.txt.  
**plotflux.apr:** plot flux vectors along the boundary of Texas cities (arow.apr) as an exercise using earlier version of atmoral.apr, plotflux.apr, and arow.apr as described at <http://www.cwr.usra.edu/cwr/realtime/cr794/atmoral/atmoral.htm>.

**PROJECT FILES**  
**atmoral.apr:** project used to make flux integration calculations; accesses files in and below the directory /Home/name/TEXAS/atmoral.  
**diverge.apr:** project used to make divergence calculations; accesses files in and below the directory /Home/name/TEXAS/atmoral.  
**OTHER TEXT OR DBASE FILES:**  
**~/atmoral/mq00.txt:** monthly qv flux for Texas boundary points at 0 UTC  
**~/atmoral/mq01.txt:** monthly qv flux for Texas boundary points at 6 UTC  
**~/atmoral/mq02.txt:** monthly qv flux for Texas boundary points at 12 UTC  
**~/atmoral/mq03.txt:** monthly qv flux for Texas boundary points at 18 UTC  
**~/atmoral/mq04.txt:** monthly qv flux for 2x2 degree grid at 0 UTC  
**~/atmoral/mq05.txt:** monthly qv flux for 2x2 degree grid at 6 UTC  
**~/atmoral/mq06.txt:** monthly qv flux for 2x2 degree grid at 12 UTC  
**~/atmoral/mq07.txt:** monthly qv flux for 2x2 degree grid at 18 UTC  
**~/atmoral/mq08.txt:** control file for the script convert.txt; specifies input and output file names, key fields, etc.  
**~/atmoral/mq09.txt:** ~/atmoral/mq10.txt: files created by the program ref1.f; contain mean monthly flux estimates for each boundary segment in kg/m<sup>2</sup>.  
**~/atmoral/mq11.txt:** ~/atmoral/mq12.txt: files created by the program ref2.f; contain mean monthly flux estimates at each 2 degree grid point in kg/m<sup>2</sup>.  
**~/atmoral/mean.txt:** file describing data provided by Allen Bales at the University of Iowa.  
**~/atmoral/theta3.txt:** results of flux integration calculation across the border of Texas; fields: year, month, inflow [mm/month], outflow [mm/month], netflow [mm/month], C1, C2, ... etc [mm/month]  
**plotdivad.txt:** output file from diverge.apr; fields are cell ID's and month in months; units are kg/m<sup>2</sup>/h; this file is used by the program convert.txt.  
**plotdivad.txt:** contains mean monthly divergence values for Texas; the field in plotdivad.txt, labeled "tot" contains average divergence estimates in units of kg/m<sup>2</sup>/h; if the values in this field are multiplied by the number of seconds in the month, the divergence in mm/month is obtained.  
**COVERAGES:**  
**~/atmoral/contigs:** point coverage of the endpoints of the boundary segments in tdrpoin.shp.  
**~/atmoral/contigs:** coverage containing line and node topology of Texas boundary segments in geographic coordinates -- used for flux integration calculation. Attributes include "L", "Y", and "T" which are the corresponding length of these segments on the Clarke 1866 ellipsoid in meters; the point coverage of segments is attributed with Cartesian coordinates which are used by the program calcflow.apr.  
**~/atmoral/contigs:** generalized border of Texas in an all-area projection with parameters used for national maps.  
**~/atmoral/contigs:** polygon coverage -- intersection of generalized Texas border (contigs) and 2 degree cell (tomb2).  
**~/atmoral/fragpt:** polygon coverage of 2 degree cells as shown in Figure 3.1 of the report; projection is all-area with parameters used for national maps.  
**~/atmoral/points:** point coverage of 2 degree by 2 degree grid points used for divergence calculation (Equation 3.7).  
**~/atmoral/points:** projected version of points.  
**tbl01p:** polygon coverage of Texas boundary, projection is all-area with parameters used for national maps.

**AVTFILES**  
**PROGRAMS:**  
**at0\_area.apr:** script used to determine the incremental drainage area of each basin delineated according to the USGS.  
**at0files.apr:** add fields to the attribute table of the delineated watershed coverage -- /Texas/basins/tomb3 and compute values for these fields.  
**check3.apr:** compare flow at outlet points in actual runoff grid with flow at gaging stations to make sure that the runoff mapping method worked. Output file is check3.txt.  
**equivpts:** list of cells with Cartesian coordinates which are used by the program calcflow.apr.  
**convert.apr:** create new fields in tomb3 with different units for flow, average rain, or drainage area, etc.  
**plotv.apr:** plot v (y) charts on selected columns in an INFO table. User is prompted to enter fields for plotting.  
**query.apr:** make a query on delineated basins in result2.apr. Singlefile making slight changes to a complicated query.  
**verttext.apr:** write a text file for specified fields in an attribute table.

**BASINS**  
**PROGRAMS:**  
**basins.apr:** describes DEM processing, including 30 second data from Mexico DEM cells.  
**basins.apr:** description of stream basins in procedure for Texas only -- prior to including the Mexico data -- many of the output grids are obsolete and these have been deleted.  
**calcflow.apr:** adds up all of the values in the flungrid created by netflow3.apr.  
**gencoord.apr:** script used to write a file containing the points of coordinates linked by the user; used to help identify the outlets of major basins.  
**inflow.apr:** script used to get information about net inflow for selected points and write the results to an INFO file (linked to a button and used interactively).  
**mapout.apr:** .amr used to generate raster grid from text file for 164 basins.  
**netflow3.apr:** program used to calculate the net flow of runoff across the border of Texas given a flowaccumulation grid, a flowdirection grid, and a grid of the Texas border.  
**out2.txt:** file containing list of outlets used to delineate 164 watersheds; created with select.apr and outflow.apr; script used to write the outflow from selected points to a table; linked to a button and used interactively.  
**plotflow.apr:** script used to plot measured flow vs. potential flow.  
**select.apr, select2.apr:** AMRL that allow the user to interactively select watershed outlets given a point coverage and a link grid.  
**OTHER TEXT OR DBASE FILES:**  
**keyatt.txt:** text file describing the key attributes of the final coverage of 164 delineated watersheds.  
**COVERAGES:**  
**at0area2:** major watersheds in Texas; taken from a CD-ROM created by Smith, 1995, and possibly re-projected.  
**at0basins:** coverages of major basins derived from 15' data (not clipped with the State boundary).  
**at0out2:** point coverage of outlets in the major basins.  
**at0out3:** coverage of 164 outlets with potential flow as attributes.  
**at0p15:** EPA's River Reach File (RRF) coverage with coastal polygons eliminated; national projection.  
**at0p15:** RRF coverage with coastal polygons eliminated; national projection.  
**at0p15:** RRF coverage with coastal polygons eliminated; national projection.  
**tomb3\_1:** polygon coverage of each one Texas border for which 2d elevation values are greater than 0; tomb3\_1 has many basins clipped out.  
**tomb3\_2:** mask of Texas border in geographic coordinates from the same data source as tomb3\_1.  
**tomb3pms:** delineated watershed boundaries in geographic coordinates.  
**tbl01c:** delineated streams at a 1000 cell threshold.  
**tbl01d:** delineated streams at a 3000 cell threshold.  
**tbl01e:** delineated streams at a 3000 cell threshold clipped by the border of Texas.  
**tomb3\_1:** basins delineated from tdrpoin and out2, the attributes of this coverage are used to select basins for the "select" runoff curve; attributes of this coverage are described in the text file keyatt.txt.  
**tomb3\_2:** tomb3\_2 in geographic coordinates.  
**GRID:**  
**demat:** portion of the U.S. 500 m DEM that covers Texas and areas draining to Texas, in national all-area projection; obtained from usdem2; starting point for delineation (see basins.apr).  
**dem2:** filled and projected 500 m DEM for Texas (see basins.apr) and for creation details).  
**dem2zmf:** filled version of the combined Mexico and Texas DEM.  
**demv:** dem2zmf resampled to a larger cell size to make it faster to display in ArcView.  
**disclip:** zeros in the stream and outlet grid on the landscape including the Mexico terrain (filled twice via demclip.apr and reproject). A few cells in disclip were edited with Gridtools to make sure that two problematic areas drained in the correct direction (see Section 5.2.1 for problem description and the solution file in this directory for solution details).  
**mapout2:** 13 major basins delineated based on user selected outlet points.  
**mapout3:** grid of outlet points for major basins.  
**netflow3:** selected portion of the North American 30 second data in geographic coordinates; notes is assigned the value NODATA.  
**out2h.txt, out2i, out2j:** text file, coverage, and grid of 164 outlet points.  
**stream:** gridmed stream of rtdrpg with a cell size and dependent consistent with the DEM (see basins.apr) and for creation details).  
**tbl01m:** delineated streams for Texas and Mexico with a 1000 cell threshold.  
**tbl01n:** gridmed streams for Texas and Mexico with 3000 cell threshold.  
**tbl01o:** gridmed streams at 300 cell threshold.  
**tbl01p:** stream data from tbl01m and tbl01n.  
**tbl01q:** flowaccumulation grid from tbl01p.  
**tbl01r:** flowaccumulation grid from tbl01p.  
**tomb3\_1:** basins delineated from out2j using tbl01m.

**EVAP**  
**PROGRAMS:**  
**at0evap.apr:** script used to reformat gross reservoir evaporation data; creates INFO file id0evap.  
**basmap.apr:** determine the appropriate reservoir evaporation basin in Texas.  
**evap.apr:** add fields of "sum\_month" and "sum\_year" to the INFO file "evapor"; "sum\_month" is the average annual EE over 1961-1990. "THE UNITS ARE ACTUALLY MM/MONTH SO FOR ANNUAL TOTAL, multiply by 12." These two values are the same for those basins that have monthly evaporation data.  
**evap2.apr:** estimate annual gross evaporation from the reservoir in reser00 and add a field ("evap") containing this information to the reservoir coverage.  
**fixquad.apr:** repair problems with polygons (Q) in first column of 1 degree quad.  
**getatt.f:** reformats gross evap estimates so that they can be loaded into ArcView; input: gv=at0evap; Output: evap2.txt.  
**mapout.apr:** create an INFO table (mapout2.dbf) that contains monthly average gross evaporation from each quadrangle.  
**plotevap.apr:** script that can be used to plot time series data.  
**quad.f:** FORTRAN program used to write general file (quad.gem) for 1 degree quad.  
**tbl01evap:** determine the appropriate reservoir evaporation from each delineated watershed.  
**tbl01evap:** FORTRAN program used to create a file with the correct quadrangle index (Q) to match Albrecht's data; input: jolink.txt; output: jolink2.txt. "ArcInfo won't assign correct user IDs so I manually changed them (I've seen this error before when generating square cells) and added a column called 'quad' to 'newtbl01' from the FORTRAN program (tbl01evap) and create jolink2.txt).  
**tbl01evap:** add the field (called year to the reservoir coverage; this is the year the reservoir was impounded -- simplify the "imp\_date" field in dam02.dbf).  
**tbl01evap:** computes the weighted average evaporation in each year and add a new field called "annual" to the INFO table evap2.  
**OTHER TEXT OR DBASE FILES:**  
**tbl01evap.dbf:** dbase file containing gross reservoir evaporation estimates on a 1 degree grid.  
**at0\_evap01:** raw data file with net reservoir evaporation from Albrecht.  
**dam02.dbf:** table containing reservoir attributes corresponding to the reservoirs in the coverage reaps; these attributes have either coverage or polygon area for reservoirs impounded before 1960 or reservoir area for reservoirs impounded after 1960.  
**gv=at0evap:** gross evaporation estimates for quadrangles covering Texas obtained from Albrecht Rodriguez (T-108) (units are inches/month). Some quads contain monthly estimates from 1940 to 1990 while others contain data from 1971 to 1990.  
**jolink.txt, jolink2.txt:** text files with used to match quadrangle index numbers in the coverage of 1 degree quadrangles.  
**quad.gem:** generate file for a point coverage at the center of each 1 degree quadrangle.  
**quad.gem:** generate file for 1 degree quad polygons.  
**INFO FILES:**  
**evapor:** contains quad-id, year, and evap, annual mean evaporation / 12 [1961-1990] -- "sum\_month" and annual mean evaporation / 12 [1971-1990]; this information is joined to quad and table.  
**evap2:** INFO table that contains reformatted gross reservoir evaporation data.  
**dam02:** INFO file containing dam attributes.  
**tbl01evap:** 30 year monthly average of gross evaporation; 12 values for each quad.  
**COVERAGES:**  
**gv=at0evap:** 1 degree quad in geographic space attributed with quadrangle index number and x,y coordinates of center point.  
**tbl01evap:** 1 degree quad in TMS all-area with these attributes:  
**year =** start year when estimates are available  
**sum\_year =** end year when estimates are available  
**sum\_month =** 30 year mean (sum/month)  
**sum1 =** 20 year mean (sum/month)  
**sum2 =** annual 30 year (or 20 year when 30 year not available) mean  
**evaporation (sum/year)**  
**quadp:** projected point coverage of the centers of 1 degree quad.  
**reserp:** polygon coverage of reservoirs in all-area projection with TMS parameters.  
**tbl01evap:** coverage of reservoirs built before 1960; field "tbl01evap" contains evaporation estimate (in<sup>3</sup>/year) based on polygon area; field "sum\_evap" contains evaporation estimate (in<sup>3</sup>/year) based on conservation area.

**LANDUSE**  
**tbl01:** landuse coverage from Smith, 1995, CD-ROM.  
**tbl01evap:** polygons in blue with LF = 1 (urban landuse types).